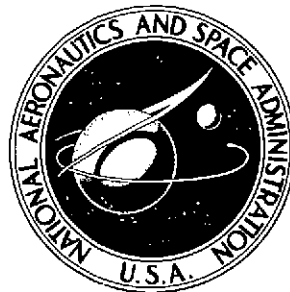


NASA TECHNICAL NOTE



NASA TN D-7898

NASA TN D-7898

(NASA-TN-D-7898) ANNEALING OF AROMATIC  
POLYIMIDE PRECURSORS (NASA) 66 P HC \$4.25  
CSCL 07C

N75-18433

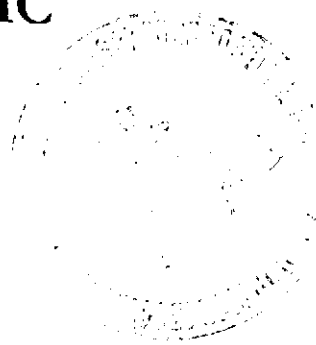
H1/27  
Unclas  
12520

## ANNEALING OF AROMATIC POLYIMIDE PRECURSORS

*N. T. Wakelyn*

*Langley Research Center*

*Hampton, Va. 23665*



1. Report No. NASA TN D-7898		2. Government Accession No.		3. Recipient's Catalog No.	
4. Title and Subtitle  ANNEALING OF AROMATIC POLYIMIDE PRECURSORS				5. Report Date March 1975	
				6. Performing Organization Code	
7. Author(s)  N. T. Wakelyn				8. Performing Organization Report No.  L-9802	
9. Performing Organization Name and Address  NASA Langley Research Center Hampton, Va. 23665				10. Work Unit No.  505-03-31-01	
				11. Contract or Grant No.	
12. Sponsoring Agency Name and Address  National Aeronautics and Space Administration Washington, D.C. 20546				13. Type of Report and Period Covered  Technical Note	
				14. Sponsoring Agency Code	
15. Supplementary Notes    This paper was part of a dissertation entitled "Solid State Polymerization and Crystallography of Polyimide Precursors" presented in partial fulfillment of the requirements for the degree of Doctor of Philosophy in Materials Science, University of Virginia, Charlottesville, Virginia, May 1974.					
16. Abstract  <p>A study has been made of the thermal behavior of polyimide precursors: an isomeric pair of crystals of the complex formed by p-phenylenediamine with the separated isomers of the di-isopropyl ester of pyromellitic acid. Specimens of this material were isothermally annealed in the temperature range 120° C to 170° C for periods of time up to 1 week. Although this temperature range is well below that customarily used for imidizations, the working hypothesis was that it would be more likely that a polymer embodying at least part of the precursor structure could be formed if the molecular motion was minimized to that actually required for the formation of the imide linkage.</p> <p>The progress of the annealing was followed by: infrared spectroscopy (IR), differential thermal analysis (DTA), powder X-ray diffraction, and thermal gravimetric analysis (TGA). The infrared measurement showed definite evidence of imidization for the longer time, higher temperature annealings. The differential thermal analysis showed that the route from precursor to polymer was characterized by two solid-state transitions. The powder X-ray diffraction showed that the material, which by the IR was clearly imide and which had completed the final solid-state transition, did, indeed, contain residual crystallinity based upon that of the starting material and thus was suggestive of a topochemical imidization. However, the TGA suggests a component of unknown nature present in these materials which began to boil off at approximately the position of the lower temperature endotherm. Since the sensitivity of the IR is such that an unreacted minor component could remain undetected and thus could possibly be responsible for the crystallinity, the case for a crystalline polymer is unproven.</p> <p>Single crystal X-ray analysis of the meta monomer yields a structure of chains of alternating acid and base and suggests that this monomer is amenable to polymerization with a minimum of geometrical disruption.</p>					
17. Key Words (Suggested by Author(s))  Polyimide precursor polymerization Topochemical Solid state			18. Distribution Statement  Unclassified - Unlimited   New Subject Category 27		
19. Security Classif. (of this report)  Unclassified	20. Security Classif. (of this page)  Unclassified	21. No. of Pages  64	22. Price*  \$4.25		

# ANNEALING OF AROMATIC POLYIMIDE PRECURSORS<sup>1</sup>

N. T. Wakelyn  
Langley Research Center

## SUMMARY

A study has been made of the thermal behavior of polyimide precursors: an isomeric pair of crystals of the complex formed by p-phenylenediamine with the separated isomers of the di-isopropyl ester of pyromellitic acid. Specimens of this material were isothermally annealed in the temperature range 120° C to 170° C for periods of time up to 1 week. Although this temperature range is well below that customarily used for imidizations, the working hypothesis was that it would be more likely that a polymer embodying at least part of the precursor structure could be formed if the molecular motion was minimized to that actually required for the formation of the imide linkage.

The progress of the annealing was followed by: infrared spectroscopy (IR), differential thermal analysis (DTA), powder X-ray diffraction, and thermal gravimetric analysis (TGA). The infrared measurement showed definite evidence of imidization for the longer time, higher temperature annealings. The differential thermal analysis showed that the route from precursor to polymer was characterized by two solid-state transitions. The powder X-ray diffraction showed that the material, which by the IR was clearly imide and which had completed the final solid-state transition, did, indeed, contain residual crystallinity based upon that of the starting material and thus was suggestive of a topochemical imidization. However, the TGA suggests a component of unknown nature present in these materials which began to boil off at approximately the position of the lower temperature endotherm. Since the sensitivity of the IR is such that an unreacted minor component could remain undetected and thus could possibly be responsible for the crystallinity, the case for a crystalline polymer is unproven.

Single crystal X-ray analysis of the meta monomer yields a structure of chains of alternating acid and base and suggests that this monomer is amenable to polymerization with a minimum of geometrical disruption.

---

<sup>1</sup>This paper was part of a dissertation entitled "Solid State Polymerization and Crystallography of Polyimide Precursors" presented in partial fulfillment of the requirements for the degree of Doctor of Philosophy in Materials Science, University of Virginia, Charlottesville, Virginia, May 1974.

## INTRODUCTION

The class of main chain aromatic polyimide polymers contains many members of great interest to the researcher and several of growing commercial importance. These materials, which are prized for their superior high temperature and radiolytic properties derived from their main chain aromaticity (refs. 1 to 4), are produced as films, enamels, fibers, and composites for such varied uses as electrical insulation, adhesives, and lubricants. They also find aerospace application as structural materials for lightweight, high-temperature service (refs. 5 to 9).

In the history of polymer science, the addition of crystalline order (one-, two-, or three-dimensional) to a polymeric system has resulted in the improvement of commercially attractive properties such as hardness, toughness, and increased tensile strength as well as increased dimensional stability in the presence of solvents (refs. 10 and 11). Procedures such as the calendering of film and drawing of fiber are used to produce such order. Since the imide polymer is subject to cross linking during polymerization and is usually fabricated in solution from multifunctional and rather bulky monomers, it is normally found in an amorphous state.

A variety of precursors of imide and pyrrone polymers have been synthesized by Bell (ref. 12), based upon the commercial synthesis of aliphatic polyamides by a salt process. He succeeded in establishing a novel route for obtaining a variety of heteroaromatic polymers, formed through a polyamide stage, by the use of these precursors. He hypothesized that since these precursors appeared to be crystalline, several of them might provide possible routes for obtaining main chain aromatic polymers in the crystalline state. Single crystals of trioxane have been polymerized in the solid state to polyoxymethylene with oriented chains (refs. 13 and 14). A variety of ring monomers have been subjected to radiation polymerization and were converted to linear polymers by a ring opening mechanism in the solid state with properties which suggest the imposition of the monomer orientation and order upon the polymer structure (ref. 15).

Crystalline organic compounds have been observed to undergo "topochemical" reactions (ref. 16) in which the process is dependent upon the geometrical relationships of the reacting groups so that not only is reaction in the liquid state different in rate and/or product from reaction in the solid state but also different polymorphic forms of the same compounds can display different chemistry (ref. 17). Although one would suppose that the production of polymerization byproducts would disrupt the crystalline order of the reacting molecular matrix as they traveled to the surface, topotactic condensation polymerization has been observed. For example, the cyclization of phthalanilic acid, with the elimination of water, is reported to be topotactic (ref. 17). The essential characteristic of topotactic polymerizations appears to be the minimization of thermal motion to that actually required for the linking up of the monomer molecules (ref. 18).

If one could polymerize a crystalline imide precursor in the solid state at a temperature at which the minimum molecular motion to achieve the imide linkage occurs, there is the possibility that the polymer would display at least part of the crystal structure of the starting material and a crystalline aromatic polyimide would be achieved. Along with the possibility of enhanced physical properties, there is the chance of gaining enough chemical and physical understanding of the process to enable one to move toward the long-term goal of the synthetic chemist of being able to tailor desired properties into his constitutions of matter. Nevertheless, solid-state polymerization holds out the possibility of constraining an array of molecules in a known and perhaps desired position until they react.

The goal of the present study was to discern the thermal behavior of a pair of isomeric, crystalline, imide precursors and possibly to achieve a polyimide polymer possessing residual crystallinity by their annealing in various ways for varying periods of time and at various temperatures. A variety of analytical tools have been used in the attempt to characterize the materials, before and after annealing, in an effort to determine what they are, what they become, and what geometrical and physical paths were taken.

#### SYMBOLS

A	geometrical structure factor
Ar	aromatic nucleus
$a, b, c$	unit cell magnitudes
B	temperature factor
E	normalized structure factor
$h, k, l$	indices of diffracting planes
$I_{\min}$	minimum measured X-ray intensity
K	scale factor
$N(Z)$	fraction of number of reflections less than a specified fraction of average intensity Z

$n$	n-glide plane
$P2_1/n$	space group 14
R	isopropyl group
$\Delta T$	temperature increment
$x, y, z$	coordinates of equipoint set
$\bar{x}, \bar{y}, \bar{z}$	negative coordinates of equipoint set
$\delta$	partial charge
$\theta$	angle of incident beam to reflecting plane
$2\theta$	angle of diffracted beam from incident beam
$\theta_m$	monochromator angle
$\lambda$	wavelength, generally expressed in Angström units

## EXPERIMENTAL ANALYSIS

In order to ascertain the possibility of synthesizing a crystalline polyimide polymer in the solid state and perhaps gaining insight into any topochemical constraints as well as achieving mechanistic understanding, such as the involvement of an amide intermediate stage, it was decided to isothermally anneal an isomeric pair of imide precursors at the lowest possible temperature required to generate a polymer. It was assumed that more highly crystalline polymers could be achieved at the lowest temperatures, in which molecular motion is minimized to that actually required for the formation of the imide linkage without destroying the crystalline order present in the precursors, or, at least to maintain some of that order in the polymer. It was recognized that this process could involve prolonged annealing times. To discern the lowest possible temperature and the required times, various temperatures and times were used until a data assemblage was generated, temperature varying in 10 C° increments from 120° C to 170° C and annealing times varying from 1 day to 1 week. Both open and sealed specimen containers were used.

The annealing was accomplished in a vacuum oven, modified by the installation of a massive aluminum block into which specimen receiving holes had been cut and thermocouples placed in the region of specimen residence. It was found that the temperature of the interior of the block could be maintained to within better than 1 C° for periods up to a week. The interior of the oven was subject at all times to outgassing by the action of an oil diffusion vacuum pump which maintained the pressure in the range of 1 torr. (1 torr = 133.322 N/m<sup>2</sup>.) The usual procedure for the insertion of a specimen involved the attaining of the desired temperature, maintaining this temperature for sufficient time to insure that it was in true equilibrium, breaking of the vacuum, and rapid emplacement of an open tube containing the preweighed specimen, closing of the oven, and reestablishing the vacuum. The mass of the container and specimen is insignificant compared with that of the aluminum heat sink. Typically, a temperature decline of 2 C° from that desired was measured for the first half hour after the insertion of a specimen. The succeeding 5 hours of annealing would be conducted at 1 C° lower than that desired, the desired temperature being reached and maintained thereafter.

It was recognized that any weight change information could be obscured, at least for the higher temperature annealing tests, by loss of reactant material as well as product material due to the combination of high temperature and low pressure. Therefore, sealed tube specimens were annealed as duplicates for some of the higher temperature, longer time tests. Specimen and container were sealed in a tube after room-temperature outgassing for 2 days under a vacuum-ion pump with a manifold pressure of  $3 \times 10^{-7}$  torr as measured by the ion gage. Typically, the bottom of the tube would be at  $5 \times 10^{-6}$  torr during the outgassing procedure.

After initial examination of the starting materials by infrared and single crystal X-ray analysis, the course of polymerization was followed for the various times and temperatures, for the two isomeric precursors, in open and sealed tubes, by measurement of weight change, differential thermal analysis, infrared spectrometry, and powder diffraction. Polymeric samples produced from the two isomers were tested by thermal gravimetric analysis.

The differential thermal analysis thermograms were taken with a programmed heating rate of 10 C°/min and standard glass beads as a reference. The single crystal X-ray data were collected with a computer-card-controlled single crystal X-ray diffractometer. The infrared spectra of the unannealed materials were taken with the dual-grating instrument whereas those of the annealed materials were taken with the prism spectrophotometer.<sup>2</sup>

---

<sup>2</sup>All IR spectra were taken on KBr disks.

## RESULTS AND DISCUSSION

### The Precursor Material

The starting materials used in this study were a pair of precursors of imide polymers synthesized from p-phenylenediamine and an isomeric pair of di-isopropyl esters of pyromellitic acid (fig. 1), separated by fractional crystallization and characterized by nuclear magnetic resonance. The materials can be named 1,4-phenylenediamine 4,6-dicarboisopropoxy-1,3-benzenedicarboxylic acid (termed the meta isomer and present in the form of pale pink needles) and 1,4-phenylenediamine 3,6-dicarboisopropoxy-1,4-benzenedicarboxylic acid (termed the para isomer and present in the form of pale pink platelets). Elemental analyses were as follows:

Element	Calculated percent $C_{22}H_{26}N_2O_8$	Found percent meta	Found percent para	Calculated percent monohydrate
Carbon	59.19	58.88	58.42	56.89
Hydrogen	5.87	5.87	5.94	6.08
Oxygen	28.69	29.03	29.95	31.00
Nitrogen	6.27	6.15	6.13	6.03

These data suggest the possibility of hydration of the para isomer, with less than 1 molecule of water per unit cell. The X-ray powder diffractograms of figure 2 show the amorphous characteristics of the polyimide produced by solution casting along with the crystalline patterns of the two isomeric precursors.

Infrared spectra (unannealed).- The meta and para isomers contain a variety of infrared active functional groups which can in various ways interfere with each other to obscure the interpretation of the respective spectra. In addition to the presence of the aromatic rings and the two isopropyl ester functional groups, there are the following possibilities:

- (a) 2 amino groups + 2 carboxyl groups
- (b) 1 amino group + 1 ammonium ion + 1 carboxyl group + 1 carboxylate ion
- (c) 2 ammonium ions + 2 carboxylate ions

In addition to harmonic interactions between the various bands, there are band shiftings due to both inter- and intra-molecular hydrogen bonding and interactional effects produced by proximity of groups relative to each other and related to the internal geometry of the respective unit cells of the crystals.

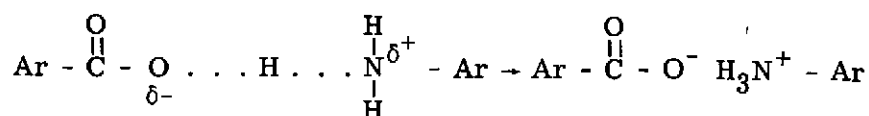
The spectra of the original, unannealed, meta material (fig. 3) contain sharp bands at  $3375\text{ cm}^{-1}$  and  $3300\text{ cm}^{-1}$  which are ascribed to asymmetric and symmetric stretch-



ing of  $\text{NH}_2$ . Both bands are shifted downward from the position of the free amino group ( $3500\text{ cm}^{-1}$  and  $3400\text{ cm}^{-1}$ ) by about  $110\text{ cm}^{-1}$  (ref. 19). The calculated position of the lower band (symmetric stretch) by use of the empirical relation of Leonard and Owens (ref. 20) is  $3302\text{ cm}^{-1}$  as compared with  $3300\text{ cm}^{-1}$  measured. The implication is that the shift to lower wave numbers is caused by the participation of the N-H groups in hydrogen bonding and/or the effect of the crystal lattice. This assignment and the substantiation produced by the calculation from the empirical relation which shows that the wave-number combination for these bands is proper for N-H stretch rules out possibility (c) for the meta isomer.

The spectra of the original, unannealed, para material contain a fairly broad band at  $3175\text{ cm}^{-1}$  with a small broad shoulder at  $3110\text{ cm}^{-1}$ . If these were N-H stretching bands, calculation from the empirical relation would yield a wave number of  $3127$  for the symmetrical stretch as compared with  $3110\text{ cm}^{-1}$  measured. Nakanishi (ref. 19, p. 156) lists a difference of  $12\text{ cm}^{-1}$  between calculated and measured as good agreement. Bellamy (ref. 21), in his discussion of amino acids (which exist as zwitterions), reports that no absorption occurs in the NH stretching region of  $3500\text{ cm}^{-1}$  to  $3300\text{ cm}^{-1}$  but that instead a single band appears in the  $3130\text{ cm}^{-1}$  to  $3030\text{ cm}^{-1}$  region which has been assigned to the  $\text{NH}_3^+$  stretching mode. Although Nakanishi reports NH band shifting of as much as  $170\text{ cm}^{-1}$  and the present meta isomer NH bands are shifted by about  $110\text{ cm}^{-1}$ , for the above para bands to be NH stretches a shift of about  $310\text{ cm}^{-1}$ , which seems excessive, would be required. However, Bellamy (ref. 21, pp. 253-254) in his discussion of intermolecular hydrogen bonds, while expressing doubt that the small downward shifting ( $<100\text{ cm}^{-1}$ ) of the NH bands in condensed phase amines are due to hydrogen bonding and, indeed, stating the possibility that they represent a solid state association, gives an absorption range of  $3320\text{ cm}^{-1}$  to  $3240\text{ cm}^{-1}$  for the association with ketonic groups,  $3300\text{ cm}^{-1}$  to  $3150\text{ cm}^{-1}$  for the association with other nitrogen atoms, and the approximate range of  $3400\text{ cm}^{-1}$  to  $3100\text{ cm}^{-1}$  for possible associated NH stretch absorptions. He also indicates that broadening of the low-frequency band implies hydrogen bonding.

The original para isomer spectra also have a broad band at about  $3400\text{ cm}^{-1}$ . This can be free  $\text{NH}_2$ , the overtone of the C=O band, or a hydrogen bonded OH stretch (ref. 19, p. 32). If this band (presumed missing from the meta isomer spectra) is hydrogen bonded OH, the implication is that there is a continuous variation of the NH stretch from that of the free amino down to the  $\text{NH}_3^+$ . The lower frequency band broadens until it disappears at complete ionization, or when the partial changes become complete, as



the present case being border line, close to a salt. Or if, as implied by Bellamy, the greatest band lowerings are produced by N-N interactions, and if this type of interaction is that required to produce the measured effect, it would be almost impossible to form a polymer from the para isomer in the solid state in the topochemical sense. Although a more subjective judgment is required than for the meta isomer, possibility (c) is also ruled out for the para isomer.

Infrared spectra of acids, obtained on solids, have shown OH absorptions occurring as broad bands over the range of  $2500\text{ cm}^{-1}$  to  $3000\text{ cm}^{-1}$ , with a main peak near  $3000\text{ cm}^{-1}$  and a satellite near  $2650\text{ cm}^{-1}$ , while lacking the free carboxyl absorption,  $3500\text{ cm}^{-1}$  to  $3600\text{ cm}^{-1}$  (ref. 21, p. 163). Both the meta and para isomers (as well as the meta and para di-isopropyl pyromellitic acid, fig. 4) lack the free OH absorption at  $3500\text{ cm}^{-1}$  to  $3560\text{ cm}^{-1}$ . The para has a satellite at  $2670\text{ cm}^{-1}$  and the meta has one at  $2610\text{ cm}^{-1}$ . Although bands in this region can be assigned to symmetric  $\text{NH}_3^+$  stretch, it is believed that they are in fact due to acid OH stretch (showing solid-state association effects) since the broad band is missing in the  $3030\text{ cm}^{-1}$  to  $3130\text{ cm}^{-1}$  region (aside from the small para shoulder at  $3110\text{ cm}^{-1}$ ) and there is only one rather than a close pair of absorptions in the  $2000\text{ cm}^{-1}$  to  $3000\text{ cm}^{-1}$  region for the two isomers. The parent diacid-diester compounds (fig. 4), which do not contain nitrogen, also absorb in this region. The band at  $2985\text{ cm}^{-1}$ , found in both isomers and their starting materials, is assigned to the isopropyl group, perhaps overlapped with an OH stretch at  $2970\text{ cm}^{-1}$ .

The meta and para isomers have highly (and equally) intense C=O stretching vibrations at  $1715\text{ cm}^{-1}$  and  $1705\text{ cm}^{-1}$ , respectively. The meta and para isomers have what appear to be intense C-O stretches (not pure C-O) (ref. 21, p. 188) at  $1095\text{ cm}^{-1}$  and  $1085\text{ cm}^{-1}$ , respectively, supposedly arising from a C-O vibration coupled with an OH inplane deformation vibration, and a doublet (more obvious for the meta isomer) near  $1250\text{ cm}^{-1}$ , supposedly characteristic of carboxylic vibration (ref. 21, pp. 170-171). Subsequent annealing, however, reveals changes in the doublet near  $1250\text{ cm}^{-1}$  with progress of imidization whereas the bands slightly below  $1100\text{ cm}^{-1}$  remain unchanged.

There are small bands in each isomer between  $1610\text{ cm}^{-1}$  and  $1550\text{ cm}^{-1}$  and between  $1400\text{ cm}^{-1}$  and  $1300\text{ cm}^{-1}$  suggestive of ionized carboxyl (ref. 21, p. 174). However, since the strongest absorptions are in the  $1700\text{ cm}^{-1}$  region (carbonyl attached to aryl nuclei), it is assumed that there is un-ionized carboxyl present in both isomers based upon the presumption that the  $1700\text{ cm}^{-1}$  band contains a contribution from carboxyl carbonyl as well as ester carbonyl (since there is only one absorption here) coupled with the facts that the case for un-ionized amine (and thus carboxyl) is more evident for the meta isomer and that these carbonyl absorptions are of comparable magnitude. It thus appears that both of the precursors lie somewhere between possibilities (a) and (b), perhaps with the meta isomer closer to (a) than the para.

For the current analysis it is assumed that both isomers exist before annealing in the un-ionized state, the meta NH stretch lowering being due to solid-state effects and perhaps weak hydrogen bonding, while that of the para being due to strong hydrogen bonding. The para isomer may contain some ionization. The spectra are cluttered and confused by circumstances such as the meta bonded OH band being lower in frequency than that of the para isomer while its C=O band at about  $1700\text{ cm}^{-1}$  is higher than that of the para isomer and its N-H stretch being virtually undisturbed in comparison with that of the para isomer. A summary of the effects leading to the assumption of no ionization is as follows:

- (1) Two N-H bands above the position of the ammonium band (which is missing) as well as absorption at about  $1620\text{ cm}^{-1}$
- (2) The highest intensity bands are the single carbonyl vibrations,  $\approx 1700\text{ cm}^{-1}$ , of virtually equal intensity for both isomers
- (3) The OH absorption in the range  $2500\text{ cm}^{-1}$  to  $3000\text{ cm}^{-1}$  for both isomers, especially the one at  $2970\text{ cm}^{-1}$ , which is also present in the diacid-diester starting material (this effect could be due to  $\text{CH}_3$ )
- (4) The doublet due to carboxylic acid vibration near  $1250\text{ cm}^{-1}$  (more obvious for the meta isomer)

Single crystal diffractometry. - In an effort to learn the starting geometry of the isomeric precursors to determine whether they could be amenable to topochemical polymerization, crystals of the two isomers were examined under a microscope while mounted to a goniometer which could be rotated during the examination. Both appeared to possess monoclinic morphology. The para isomer was present as extremely thin plates whereas the meta isomer, although consisting of small crystals, was rod-like and thus more amenable to diffraction analysis.

A small meta single crystal was selected and precession camera photographs with Ni-filtered  $\text{CuK } \alpha$  radiation showed that it belonged to the monoclinic space group 14 (systematic absences:  $h0l$  with  $(h + l)$  odd,  $0k0$  with  $k$  odd). The axes were defined so that the space group was  $\text{P}2_1/n$  in order to obtain a unit cell with a  $\beta$ -angle close to  $90^\circ$ . Although this orientation is very common in the crystallographic literature for organic crystals, it is nonstandard from the viewpoint of the International Tables for X-Ray Crystallography (ref. 22) and the following equipoint set and geometrical structure factors were calculated for  $\text{P}2_1/n$ :

$$x, y, z$$

$$\bar{x}, \bar{y}, \bar{z}$$

$$\bar{x} - \frac{1}{2}, \quad y + \frac{1}{2}, \quad \bar{z} - \frac{1}{2}$$

$$x + \frac{1}{2}, \quad y - \frac{1}{2}, \quad z + \frac{1}{2}$$

$$A = 4 \cos 2\pi(hx + lz) \cos 2\pi ky \quad ((h + k + l) \text{ even})$$

$$A = -4 \sin 2\pi(hx + lz) \sin 2\pi ky \quad ((h + k + l) \text{ odd})$$

If an acid-base pair is known, the equipoint set would spread them in an alternating fashion through all space.

The intensities of a quadrant of reflections were measured ( $h$ : 11 to -12;  $k$ : 28 to 0;  $l$ : 5 to 0) out to  $\sin \theta/\lambda = 0.4736$  (by use of Mo-radiation). A graphite monochromator was used with a setting angle of  $11.52^\circ$  ( $2\theta_m$ ). To check electronic and crystal stability during the period of data collection, the intensities of standard reflections (200, 080, 002) were measured every 60th reflection. No systematic variation was observed for these standard intensities. The master card program for the diffractometer provided the following unit cell data:

$$a = 12.7127 \text{ \AA}$$

$$b = 30.1615 \text{ \AA}$$

$$c = 6.0594 \text{ \AA}$$

$$\text{Beta} = 101.53^\circ$$

$$\text{Volume} = 2276.50 \text{ \AA}^3$$

The X-ray density of the meta crystal, calculated from these measured unit cell parameters for four acid-base pairs per cell, is 1.30 g/ml as compared with 1.22 g/ml by commercial flotation analysis. (Commercial analysis for the para isomer: 1.57 g/ml.)

An overall isotropic temperature factor ( $B = 1.986$ ) and scale factor ( $K = 15.9142$ ) were calculated by using a Wilson plot contained in the NORMSF overlay of the X-Ray System of Crystallographic Programs (designated CRYSPAK). (See ref. 23.) Of the 2350 recorded reflections, 70 are systematically extinct, leaving 2280 of which 1494 are designated observed reflections and 786 "less-thans" (ref. 24). Measured intensity varied from 0 to 2972 and relative structure factors varied from 0.38 to 24.1. The highest intensity reflection was 080 and implied that the eight planar benzene nuclei were arranged

normal to be b-axis and this value is in accord with the magnitudes of the unit cell dimensions. Table I contains the statistics and distribution for the normalized structure factors  $E$ .

TABLE I.- STATISTICS AND DISTRIBUTION OF NORMALIZED  
STRUCTURE FACTORS

[ $|E1|$  is calculated with an overall scale factor whereas  $|E2|$  is calculated with scale factors representative of different intervals of  $\sin^2 \theta/\lambda^2$ .  
 $|E3|$  and  $|E4|$  are  $|E1|$  and  $|E2|$ , respectively, with anisotropic corrections applied.]

Average value	Theoretical		Experimental							
	Centric	Acentric	$ E1 $		$ E2 $		$ E3 $		$ E4 $	
$ E $	0.798	0.886	0.706		0.559		0.706		0.556	
$ E^2 $	1.000	1.000	1.000		1.021		1.000		1.018	
$ E^2 - 1 $	.968	.736	1.060		1.356		1.061		1.354	
$ E  > 3.0$	.27	.01	12	.51	43	1.87	8	.33	38	1.67
$ E  > 2.5$	1.24	.19	34	1.45	76	3.32	33	1.45	74	3.25
$ E  > 2.0$	4.55	1.83	110	4.77	161	7.02	108	4.72	160	6.97
$ E  > 1.8$	7.19	3.92	165	7.20	227	9.87	172	7.51	215	9.38
$ E  > 1.6$	10.96	7.73	262	11.48	303	13.19	260	11.39	287	12.54
$ E  > 1.4$	16.15	14.09	377	16.51	369	16.09	368	16.15	355	15.46
$ E  > 1.2$	23.01	23.69	531	23.26	466	20.34	533	23.37	457	19.96
$ E  > 1.0$	31.73	36.79	724	31.71	593	25.94	722	31.66	588	25.74
$ E  > 0.0$	100.00	100.00	2280	100.00	2280	100.00	2280	100.00	2280	100.00

Before the X-Ray System of Crystallographic Programs (CRYSPAK) was obtained, a series of computer programs, including those for data reduction, Wilson plot and zero moment test, Fourier, and Patterson Map, were written. The data reduction program contained the correction for monochromator angle to the Lorentz and polarization corrections (ref. 25). The result of the zero moment test (ref. 26), which involves the determination of the fraction  $N(Z)$  of the reflections less than a specified fraction of the average intensity and which is based upon the fact that centrosymmetric crystals tend to have more weak or unobserved reflections than noncentrosymmetric ones, is shown in

figure 5 along with the theoretical distributions. It is concluded that the calculated distribution of intensities more nearly matches that of the theoretical curve for the centrosymmetric case.

The in-house data reduction program generated the following statistics and distribution of normalized structure factor information as compared with the CRYSPAK generated information in table I:

	A	B
Average value of $ E $ . . . . .	0.611	0.688
Average value of $ E^2 - 1 $ . . . . .	0.942	0.896
$ E  > 1.0$ . . . . .	25.00	24.11
$ E  > 2.0$ . . . . .	2.50	2.34
$ E  > 3.0$ . . . . .	0.30	0.30

where A is the zero intensity data left as zero and B is the zero intensity data expressed as  $I_{\min}/3.0$  (ref. 24). The general implication of this result, coupled with table I, is that the data possesses a centric distribution or perhaps even hypercentric distribution (ref. 27), the latter conclusion being challenged by the zero moment test. (See fig. 5.)

Preliminary to the use of direct methods, a mechanized trial-and-error scheme based upon a modified ORFLS (ref. 28) program was employed. As mentioned previously, there is reason to believe that at least one of the six-membered rings was parallel, or almost so, to the  $ac$  plane. The subset of  $h0l$  data was used to find the minimum residual position for a ring, oriented with respect to the  $x$ -axis, in this plane. The minimum residual positions of arbitrarily oriented rings in  $ac$  space are shown in figure 6. The other half of the cell face is produced by the indicated centers. The minimum residual obtained in  $xyz$  space, using the fact that the origin of this space group can be moved to any center to reduce the computation, for the rings taken pairwise, is for the following position:

	x	y	z		x	y	z
1A	-0.00747	0.07825	0.84825	1B	0.24267	0.19429	0.59741
2A	.02840	.07825	.64477	2B	.27854	.19429	.39393
3A	.13812	.07825	.64477	3B	.38826	.19429	.39393
4A	.21199	.07825	.84825	4B	.46213	.19429	.59741
5A	.17612	.07825	1.05173	5B	.42626	.19429	.80089
6A	.06640	.07825	1.05173	6B	.31654	.19429	.80089

where 1A . . . 6A and 1B . . . 6B from rings A and B denote atoms from the mechanized trial-and-error schemes. Application of the two-fold screw and the n-glide would spread eight rings in a reasonable manner along the long  $y$ -axis based upon the measured minimum residual positions at  $y = 0.07825$  and  $y = 0.19429$ . Unfortunately, this trial structure, representing 12/32 of the whole, failed to refine with application of the standard Fourier methods; however, the ring at  $y = 0.19429$  did reorient with respect to the  $x$  and  $y$  axes so as to be recognizable in this new position in various direct methods E-maps. Also, the general drift of matter in the E-maps corresponds to that observed in this trial-and-error process by molecules A and B.

The centrosymmetric direct methods programs used were the PHASE overlay of CRYSPAK and the LONGS (ref. 29) multiple solution computer program, based on the reiterative application of Sayre's equation (ref. 30). After much variation of the parameters of the various direct methods programs, similar E-maps were obtained. All calculations from intensity data to final E-maps for the CRYSPAK study were made with the various overlayed programs of CRYSPAK whereas all calculations with the exception of the LONGS phasing for the LONGS study were with in-house written programs. Rings taken from the two independent studies are as follows:

CRYSPAK				LONGS			
	$x$	$y$	$z$		$x$	$y$	$z$
1C	0.26542	0.20947	0.57222	1L	0.26486	0.20000	0.53526
2C	.33232	.19087	.38889	2L	.32187	.20074	.37731
3C	.44781	.20333	.51006	3L	.43849	.22785	.49949
4C	.48373	.19855	.72756	4L	.48333	.20833	.72917
5C	.43133	.20128	.86677	5L	.41814	.19167	.84105
6C	.31833	.19776	.78312	6L	.29461	.22346	.76786

where 1C . . . 6C denote atoms from CRYSPAK E-map and 1L . . . 6C denote atoms from LONGS study. The coincidence of a ring at  $y \approx 0.20$  between the direct methods and the trial-and-error method was encouraging; however, the E-maps suggested that the other molecule ( $y \approx 0.08$ ) was not parallel to the  $ac$  plane but was roughly parallel to the  $y$ -axis, although oriented in  $x$  and  $z$  along the drift line of molecules A and B of the trial-and-error calculation. This molecule apparently extended from  $y \approx 0.06$  almost up to the one at  $y \approx 0.20$ . This would make chemical sense in that an infinite chain of alternating acid and base parts would extend through the material in proper position to "zip" up to form a polymer. It was also presumed that this lower (in  $y$ ) molecule was a pyromellitic ester and thus the molecule at  $y = 0.20$  is a phenylenediamine.

Coordinates of the nuclear carbon atoms of the lower molecule, taken from the CRYSPAK E-map (designated P1 . . . P6), are given below along with those of the four

nuclear-bonded side chain carbons (designated C2 . . . C6):

	x	y	z		x	y	z
P1	0.84917	0.16726	1.03125	C2	0.69769	0.15942	1.13237
P2	.76919	.13401	1.05704	C3	.69769	.06250	1.15972
P3	.76413	.08956	1.02431	C5	.97911	.06235	.69514
P4	.83199	.05951	.94384	C6	.97193	.17622	.71278
P5	.91649	.08686	.88715				
P6	.89896	.13440	.84954				

These coordinates together with those of the upper molecule would refine with ORFLS least-squares value to a residual of about 0.4. This result is indicative of much error in the trial structure.

The regions of the E-maps where the two molecules were chosen presented a multiplicity of choices for benzene rings overlapping, the apex of one ring being in the center of another while sharing two other carbons. The geometry of the positions of the two nitrogen atoms in the upper molecule and the four carbon atoms in the lower molecule fell in with the overlapping pattern. Calculations of the residual for a large variety of alternate rings failed to provide a better choice of trial structure. Use of the TANGEN overlay of CRYSPAK, which allows biasing of the sign determination by specifying certain signs from a structure factor calculation from atom input, only produced substantially similar E-maps at best. Choices of nitrogen atoms for the upper molecule could not be made because of lack of sensitivity of the residual calculation and the ambiguity of the ring locations. Atom locations for the ester and acid oxygen and carbon atoms could be made in reasonable positions and did lower the residual, but did not refine it satisfactorily. The answer appears to lie in the fact that E-maps which fail to produce refinable trial structures often yield a correct asymmetric unit, but one incorrectly aligned with the origin. (See refs. 31 to 33.)

To detach the calculation from a choice of origin, an extra quadrant of data was generated by use of the monoclinic mirror and calculations begun, also by using the TANGEN overlay, in the space group P1. Groups of atoms, rings, pairs of rings, and alternates were all input. An input ring, in addition to itself would produce its shifted alternate, both in the input volume and in volumes produced by inherent symmetry operations. It was evident that the data contained inherent *n*-glide planes and screw axes, shifted slightly, but basically as had been presumed. Since alternate overlayed rings were always produced and since the least-squares method proved to be too insensitive to discriminate between them, the problem proved to be intractable within the context of the available resources.



The implication of this single crystal diffraction study of the meta isomer is that the asymmetric unit contains a pyromellitic acid-ester and a phenylenediamine molecule, roughly as defined by the given coordinates, molecular relationships within the unit being approximate, but descriptive, but the relationship of the unit pair to the origin being unknown. Single crystal X-ray analysis of the meta monomer yields a structure of chains of alternating acid and base and suggests that this monomer is amenable to polymerization with a minimum of geometrical disruption. A representation of this structure is shown in figure 7.

### The Polymerization Process

The course of the polymerization of the two isomeric precursors was followed by weight change, infrared spectroscopy, and powder diffractometry. The idealized reaction is shown in figure 1. That the reaction proceeded through loss of water and isopropyl alcohol was established independently by means of gas chromatography. That water and alcohol loss is characteristic for thermal treatment of compounds of this type was established by Young (ref. 34).

Weight change. - The complete reaction from the complexes of the diacid di-isopropyl esters of pyromellitic acid and phenylenediamine, with the loss of 2 moles of water and 2 moles of isopropyl alcohol per mole of precursor to produce the polyimide polymer, would result in the loss of about 35 percent of the mass of the specimen. Figures 8(a) and 8(b) display the percent loss of mass as a function of time for the isothermal annealing, at the various temperatures and containment conditions, of the meta and para isomers, respectively.

The weight change data of the two isomers are similar, the 150° C annealings leveling with time slightly below the 35 percent complete reaction line (dotted lines in figs. 8(a) and 8(b)). After 1 to 3 days at temperatures above 150° C for the open tube specimens, there is material loss higher than that required for complete reaction and thus indicates a loss of reactant material. Sealed tube specimens were annealed in an attempt to obtain data covering the higher temperature, longer time annealings without reactant material loss. The annealing of these specimens for 160° C to 170° C produces percent weight losses between the 120° C to 130° C open tube cases. However, the presence of water and alcohol above the polymerizing material should tend to establish an equilibrium condition rather far removed from complete polymerization. There is, in general, increased loss with temperature and increased loss with time until about 3 days, at which time reaction involving water and alcohol loss is substantially complete.

The trend with time of the percent weight loss data of figures 8(a) and 8(b) for the 130° C, 140° C, and 150° C annealings for both isomers appears to be of the form described by Barrer (ref. 35) as representing parabolic diffusion. To test this trend, linear regres-

sion analysis of the percent weight loss data as a function of the square root of time in hours was performed for the para and meta (130° C) specimens up to 120 hours. An adequate linear relationship was found as can be seen by the following least-squares-determined coefficients and goodness-of-fit parameters:

	Para	Meta
Intercept . . . . .	-0.3653	-0.4757
Slope . . . . .	2.513	2.532
Sample correlation coefficient . . . . .	0.9864	0.9884
Standard error of estimate . . . . .	1.722	1.603

The implication is that the reaction in this low-temperature range is diffusion controlled.

Differential thermal analysis.- Tracings of the DTA thermograms of the open tube annealings of the para isomer from 120° C to 170° C are displayed in figure 9. Figure 10 displays tracings of the DTA thermograms of the open tube annealings of the meta isomer from 120° C to 170° C. Comparison of the magnitudes of endothermic absorption is possible on the same curve but not between different curves.

The DTA data of figures 9 and 10 appear to be a series of single- or double-fusion endotherms. Such is not the case. In the usual melting-point determination in which the specimen is inspected visually as the temperature is increased, no melting is observed to occur for either annealed or unannealed specimens. At temperatures from 100° C to 105° C, the unannealed para specimen appeared to try to melt in that it in part assumed the shape of the capillary tube and in part shrunk away from the tube and appeared to shimmer without actually melting. Near 150° C, both isomers underwent faint color changes toward red. Near 175° C, the para isomer appeared to have crystallized in the sense that it had the grainy appearance of a crushed inorganic. At this temperature, the meta isomer was a brilliant deep red. At 190° C, both isomers were a rust brown. Above 190° C, the meta isomer had the appearance of a hard irregularly shaped, chunky material whereas the para filled the tube and had a porous appearance.

The DTA thermogram of the unannealed para isomer is characterized by one endotherm whose minima occurs slightly above 200° C whereas the unannealed meta isomer, also displaying one endotherm, has its minima slightly below 200° C. An attempt at an instant melting point, in which the material is deposited upon a stage which has been preheated to the desired temperature, leads to melting with decomposition at about 200° C for both isomers and is followed by solidification. Melting with decomposition is defined as a frothy melt with evident evolution of gas and change in color. The pale pink crystals produced a red frothy liquid which immediately changed to a brown solid.

The para isomer, when heated for 24 hours at 120° C, displayed a major DTA endotherm near 205° C with a slight indication of a second endotherm at 235° C. After

168 hours at the same temperature, the DTA produces two endotherms, one near 205° C and another near 235° C, the lower temperature endotherm being of slightly greater magnitude. (See fig. 9.) The 24-hour (120° C) meta case produces one major endotherm near 197° C, whereas the 168-hour specimen (120° C) produces two endotherms, one near 195° C and another near 220° C, the lower temperature endotherm being two to three times the size of the higher temperature one. (See fig. 10.) Since the 120° C 24-hour thermograms are similar to those of the respective unannealed isomers (with the exception of the slight indication of the second endotherm for the para isomer), it is evident that the chemical and physical changes responsible for DTA changes occur slowly and require several days at this temperature, and that the para isomer is changing faster than the meta isomer.

Since melting is not occurring at this lowest annealing temperature, it is assumed that two solid-state transitions are occurring for each isomer, the second transition at the higher temperature in each case being possible only after prolonged annealing has produced enough change in the material. That is, the endotherms are associated with solid-state transitions which occur consecutively within a defined volume of the material.

Annealing at temperatures from 120° C to 170° C produces changes in the DTA endotherms in the range 195° C to 250° C. There is, in general, an exchange between time and temperature — longer times at a lower temperature being equivalent to shorter times at a higher temperature. In the 130° C to 140° C annealings there are two endotherms for the shorter times and only the higher temperature endotherm for the longer times, the para isomer appearing to have undergone more change at specific time-temperature intervals. All specimens in the 150° C to 160° C temperature range are characterized by their particular high-temperature endotherm only. In the 170° C annealings there is the trend with time of loss of the higher temperature endotherm, the meta isomer showing complete loss at 120 hours, the para almost complete loss. In the sealed tube annealings for 168 hours, 160° C and 170° C, both endotherms are completely missing for the meta isomer and only a slight indication of the higher temperature endotherm is noticeable for the para isomer. (See fig. 11.) The para isomer appears to change more rapidly initially than the meta, but the meta appears to change more completely.

Since there are two transitions and two gaseous products involved in the polymerization, one might tend to associate a transition with the endothermic production and evolution of gas. However, model compound studies of similar materials (the same diacid-diester but with tetrafunctional amines) have shown the elimination of water and alcohol to occur simultaneously (ref. 34). The previously cited work and another work (ref. 12) indicate that meta-oriented salt intermediates react to produce a polymer at slightly lower temperatures than the para intermediates in accord with the present finding of the relative positions of the lower temperature endotherms.

Infrared spectra (annealed).- The qualitative successive changes of the precursors at various stages of annealing are shown in the reproductions of the records from the prism spectrophotometer in figures 12 to 25. Infrared bands characteristic of the imide ring are reported to be the C-N at  $1380\text{ cm}^{-1}$ , the C=O doublet at  $1780\text{ cm}^{-1}$  and  $1720\text{ cm}^{-1}$ , and a band of unexplained origin at  $720\text{ cm}^{-1}$  (ref. 36). (Ref. 36 cites work done by L. J. Bellamy, S. Nishizaki, A. Fukami, J. H. Freeman, and others.) These bands are present in the spectra of phthalimide, which is a model compound representative of a single link of the polyimide structure. They are present in pyromellitic dianhydride (PMDA), with a shifting downward in wave number for the  $720\text{ cm}^{-1}$  band, and including the  $1380\text{ cm}^{-1}$  band, of different shape, even though this compound has bridged oxygen. They are not present in phenylenediamine, one of the parent compounds of the precursor isomers. (See fig. 26.) These imide bands are not present in the parent di-isopropyl pyromellitic acid compounds (fig. 4) with the exception of the band at  $1380\text{ cm}^{-1}$  which appears as a sharp spike similar in appearance to that present in PMDA. It appears that the  $1380\text{ cm}^{-1}$  band is a poor choice to follow the formation of the imide ring and, if used for such purpose, must be rather broad.

Infrared evidence for the imide ring system appears in the lowest temperature para annealings. Although missing in the 24-hour,  $120^{\circ}\text{C}$  annealing, imide bands occur in the 168-hour spectrum for this temperature as a small shoulder at  $1780\text{ cm}^{-1}$  and a small but distinct peak at  $720\text{ cm}^{-1}$ . (See fig. 12.) For the  $130^{\circ}\text{C}$  annealings (fig. 13) there is slight indication for the  $720\text{ cm}^{-1}$  absorption at an even 24 hours, but a definite presence at 72, 120, and 168 hours. The  $1780\text{ cm}^{-1}$  absorption is an illusion at 72 and 120 hours at this temperature but definite at 168 hours along with the  $1720\text{ cm}^{-1}$  absorption. The  $1720\text{ cm}^{-1}$  absorption is a poor one to follow in these spectra since it occurs at the bottom of the intense carbonyl absorption and is obscured in several of the presented spectra by the wrong choice of attenuation for the concentration of absorbing material in the optical path. Imide absorption is definite at  $720\text{ cm}^{-1}$  and  $1780\text{ cm}^{-1}$  for the para precursors annealed at  $140^{\circ}\text{C}$  and above (figs. 14 to 18) for all annealing times, especially the sealed tube specimens (fig. 18) in which the absorptions at  $1380\text{ cm}^{-1}$  and  $720\text{ cm}^{-1}$  rival the carbonyl in magnitude. In a spectrum of solution cast para film, the  $720\text{ cm}^{-1}$  and  $1380\text{ cm}^{-1}$  absorptions appear with magnitude equivalent to that of the carbonyl whereas a spectrum of film, post-treated by annealing in vacuo at  $300^{\circ}\text{C}$  for 1 hour, displays a  $720\text{ cm}^{-1}$  absorption reduced in magnitude with respect to that of the  $1380\text{ cm}^{-1}$  and carbonyl absorptions. (See fig. 27.)

There is no definitive evidence of the imide ring in the infrared spectra of the meta precursor for specimens annealed at  $120^{\circ}\text{C}$  (fig. 19). There is slight indication of the  $720\text{ cm}^{-1}$  absorption in specimens of this isomer annealed at  $130^{\circ}\text{C}$  for periods of time equal to or greater than 72 hours. (See fig. 20.) There is indication of the  $720\text{ cm}^{-1}$  absorption, but not of the other imide ring bands, in the  $140^{\circ}\text{C}$  spectra (fig. 21) and com-

parable  $720\text{ cm}^{-1}$  absorption, with slight indication of  $1780\text{ cm}^{-1}$  absorption in the  $150^\circ\text{ C}$  meta spectra (fig. 22). It is only in the 168-hour  $160^\circ\text{ C}$  meta spectrum that absorption comparable with that of the para isomer is observed. (See figs. 16 and 23.) The spectra of the open tube  $170^\circ\text{ C}$  meta specimens (fig. 24) and that of the sealed tube specimens (fig. 25) yield as much, or more, indication of the imide ring as the corresponding para isomer spectra (figs. 17 and 18). In fact, the only spectra indicating complete reaction, as revealed by the loss of the isopropyl absorption at  $2985\text{ cm}^{-1}$ , are the meta  $170^\circ\text{ C}$  72- and 120-hour specimens and the sealed tube specimens of both isomers. If the requirement for complete reaction is the complete loss of absorption near  $3000\text{ cm}^{-1}$ , the only specimens which are wholly polyimide in this sense are the sealed tube meta isomers and the 120-hour  $170^\circ\text{ C}$  meta isomer. Thus, although imidization, as judged from infrared spectra, appears to proceed more rapidly initially for the para isomer, it is only the meta formulation which attains complete imidization.

If an amide had been formed as a stable intermediate, a carbonyl absorption should occur near  $1650\text{ cm}^{-1}$  (the amide I band (ref. 21, p. 205)), perhaps evidenced as a splitting of the  $1720\text{ cm}^{-1}$  imide carbonyl absorption toward a lower wave number. There is what appears to be a splitting of the carbonyl in the longer time higher temperature specimens but a definitive assignment cannot be made since it occurs in the region of the  $1720\text{ cm}^{-1}$  imide band. None of the specimens display an unambiguous amide I band. The NH absorptions above  $3000\text{ cm}^{-1}$  persist in the  $120^\circ\text{ C}$  para specimens and in the 24-hour  $130^\circ\text{ C}$  specimen and no others. In the spectra of the meta specimens, the NH absorptions are more persistent. They are present in all of the  $120^\circ\text{ C}$  specimens but only in the  $130^\circ\text{ C}$  specimens annealed up to 72 hours. This result is in keeping with the present findings which imply that imidization occurs more rapidly initially in the para isomer. With the disappearance of the NH absorption, there appears to be a broadening in the  $3000\text{ cm}^{-1}$  region and a doubling in the  $2500\text{ cm}^{-1}$  to  $2800\text{ cm}^{-1}$  region that is suggestive of the participation of a salt form as an intermediate but the doubling is present in the di-isopropyl pyromellitic acid starting materials and the broadening is subjective since the curve is continuous through the former NH region.

Powder diffractometry. - The diffraction patterns of the annealed specimens were taken in an attempt to record the indication of structural changes as a function of time and temperature of annealing. Annealing at the higher temperatures for periods of time around a day appears to introduce complexity into the diffractograms, perhaps an indication of formation of a polymorph. Longer annealing produces a simplification of the diffractograms, perhaps indicative of loss of order and/or transformation of polymorph into a polymer, but what remains basically embodies the pattern of the starting material and in this sense indicates changes of a topochemical nature. Illustrative of this change is that recorded for the  $170^\circ\text{ C}$  specimens. (See figs. 28 to 30.)

It is observed that the broad diffraction band in the  $20^\circ$  ( $2\theta$ ) position of the solution cast material (fig. 2) is still represented in the  $170^\circ$  C 120-hour specimens of both isomers, which have definite imide characteristics, by more than one differentiable peak. This result would have to be interpreted by the usual methods of crystallinity determination by X-ray diffractometry (refs. 37 to 39), in which the specimen is mathematically positioned between maximum and minimum crystallinity diffraction patterns, as containing residual crystallinity. In addition to this region there are peaks in the diffractograms for these specimens in regions where the solution-cast material displays a flat background.

Comparison of DTA and IR spectra.- A comparison of the time-temperature data for the onset of loss of the first and second DTA endotherms with infrared spectral data denoting the appearance of definite imide bands and complete loss of ester character follows for the open tube specimens:

Temperature, $^\circ$ C	Loss of first endotherm	Loss of second endotherm	Imide bands	Complete loss $\approx 3000\text{ cm}^{-1}$
Para				
120	-----	-----	---	-----
130	72 to 120 hr	-----	---	-----
140	48 to 72 hr	-----	X*	-----
150	<24 hr	-----	X	-----
160	<24 hr	-----	X	-----
170	<24 hr	-----	X	-----
Meta				
120	-----	-----	---	-----
130	72 to 120 hr	-----	---	-----
140	48 to 72 hr	-----	---	-----
150	<24 hr	-----	---	-----
160	<24 hr	-----	X	-----
170	<24 hr	72 hr	X	72 hr

\*Observed.

### Polymer

One common method of estimating the high-temperature performance of a polymer is thermal gravimetric analysis (TGA), in which specimens are heated in air and/or in vacuo and their weight change with time and temperature recorded. The air TGA can be thought of as a measurement of crystallinity since weight loss can be associated with ease

of diffusion of oxidant into the material and ease of diffusion of oxidation products out of the material. Thus a well-ordered and tightly packed lattice, in effect a crystalline one, should display less reducing surface area to the oxidant.

Another use of the TGA is the estimation of the degree of conversion of a polymeric system or of the amount of curing which has been achieved. In this instance, material not built into a polymer structure would be expected to boil off before the polymer decomposes thermally. Figure 31 displays the weight fraction lost as a function of temperature for meta and para specimens annealed in open tubes at 170° C for 72 hours and in sealed tubes at 160° C and 170° C for 168 hours. In all cases the meta material appears to be the more highly cured material, although there is not much difference in the TGA behavior of the two isomers for the specimens annealed in sealed tubes at 170° C.

There is, in general, more conversion into polymers with time and temperature. There are, however, basic differences in the TGA behavior between open and sealed tube annealings. Uncured material begins to boil off the sealed tube specimens at  $\approx 150^{\circ}$  C whereas there is no appreciable loss in the open tube annealed specimens until a temperature of  $\approx 200^{\circ}$  C is reached. All sealed tube material is completely vaporized before a temperature of  $600^{\circ}$  C is reached. At this temperature there is about 40 percent of the meta and about 20 percent of the para material remaining for the open tube annealed specimens.

### CONCLUDING REMARKS

A study has been made of the thermal behavior of polyimide precursors: an isomeric pair of crystals of the complex formed by p-phenylenediamine with the separated isomers of the di-isopropyl ester of pyromellitic acid. Specimens of this material were isothermally annealed in the temperature range  $120^{\circ}$  C to  $170^{\circ}$  C for periods of time up to 1 week. Although this temperature range is well below that customarily used for imidizations, the working hypothesis was that it would be more likely that a polymer embodying at least part of the precursor structure could be formed if the molecular motion was minimized to that actually required for the formation of the imide linkage.

The progress of the annealing was followed by: infrared spectroscopy, differential thermal analysis, powder X-ray diffraction, and thermal gravimetric analysis. The infrared measurement showed definite evidence of imidization for the longer time, higher temperature annealings. The differential thermal analysis showed that the route from precursor to polymer was characterized by two solid-state transitions. The powder X-ray diffraction showed that the material, which by the infrared analysis was clearly imide and which had completed the final solid-state transition, did, indeed, contain residual crystallinity, based upon that of the starting material and thus is suggestive of a topochemical imidization. However, the thermal gravimetric analysis suggests a component

of unknown nature present in these materials which began to boil off at approximately the position of the lower temperature endotherm. Since the sensitivity of the infrared analysis is such that an unreacted minor component could remain undetected and thus could possibly be responsible for the crystallinity, the case for a crystalline polymer is unproven.

The differential thermal analysis of this material reveals two endotherms, the lower temperature one disappearing with time before the higher temperature one. It is perhaps possible to correlate the X-ray and differential thermal analysis data since one way to achieve the planar imide linkage would be to have a base nuclei drop between two acids and then rotate into the same plane. Whatever the sequence and whether one or both nuclei move, there are two endotherms and two required motions, lateral and rotational.

The reaction, at the lower temperatures, which appears to be essentially complete after 3 days as judged by weight loss does not yield the imide spectra, implies the necessity of longer annealing times and higher temperatures for the purpose of solid-state rearrangement. At the lower temperature ( $130^{\circ}\text{C}$ ), the chemical reaction appears to be governed by a parabolic diffusion rate.

A comparison of the time-temperature data for the first and second endotherms shows that it is only the meta isomer which sustains complete loss of both the differential thermal analysis endotherm and the  $3000\text{ cm}^{-1}$  infrared absorption.

By following the analogy of the amide salt process for nylons, evidence of an amide stage was expected in the infrared spectra for at least some time-temperature annealings. No unequivocal evidence for the involvement of an amide stage was found although there is evidence of the possible participation of a salt intermediate. Moreover, the meta and para starting materials appear not to be salts in the unannealed solid state. However, there is evidence for a partial ionization of the para isomer, which may explain the observation of a more rapid initial imidization for this material.

It had also been thought that water and alcohol above the polymerizing material in a sealed tube would establish an equilibrium characterized by a lower degree of polymerization than a similar case in which product molecules are continuously removed from the reaction region. On the basis of this study, it is now felt that sealed tubes at higher temperatures produce a polymer that is at least as highly polymerized as that produced in unsealed tubes without the wasteful loss of material other than water and alcohol. However, the polymerized material produced in sealed and open tubes is different in that thermal gravimetric analysis shows that they contain low boiling trace materials that are removed at different temperatures and that the open tube material appears to be more thermally stable.

The different isomers transform at different rates and through different intermediates toward the imide. This transformation must be a function of the geometry of the



isomers in the solid state which is determined by the position and characteristics of the side chain, in this case, the isopropyl group. Chemical variation of the side chain can, in principle, produce different end products.

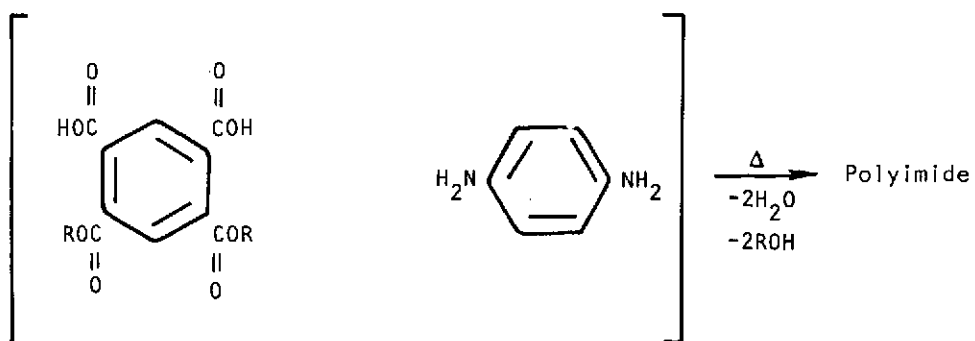
Langley Research Center,  
National Aeronautics and Space Administration,  
Hampton, Va., January 30, 1975.

## REFERENCES

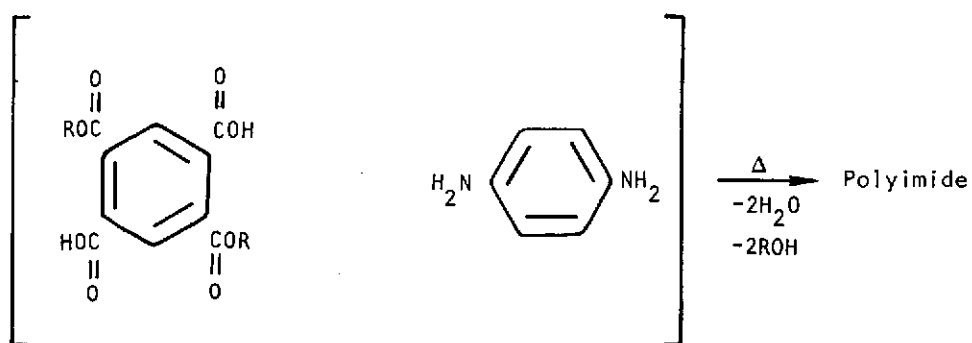
1. Charlesby, Arthur: Atomic Radiation and Polymers. Pergamon Press, Inc., 1960.
2. Pezdirtz, G. F.: Polymers for Spacecraft. Mod. Plastics, vol. 40, no. 12, 1963, pp. 123, 125-126, 128, 132, 134.
3. Kelble, J. M.; and Bernados, J. E.: High Temperature Nonmetallic Materials. Aerosp. Eng., vol. 22, no. 1, Jan. 1963, pp. 56-75.
4. Marvel, C. S.: Polyaromatic Heterocycles. Paper presented at American Chemical Society Division of Polymer Chemistry Meeting (Philadelphia), vol. 5, no. 1, Apr. 1964, pp. 167-177.
5. Bilow, Norman; and Rose, Kenneth L.: High Temperature Electrical Wire Coatings. AFML-TR-69-111, Part II, U.S. Air Force, Aug. 1970. (Available from DDC as AD 873 310.)
6. Arvay, E. A.; and Aponyi, T. J.: The Development of High Temperature Stable Polyimide Structural Adhesives. AFML-TR-71-3, U.S. Air Force, Apr. 1971.
7. Campbell, M.; and Hopkins, V.: Development of Polyimide Bonded Solid Lubricants. Lubrication Eng., vol. 23, no. 7, July 1967, pp. 288-294.
8. Standage, A. E.; and Turner, W. N.: A High-Temperature Polyimide Reinforced With Silica Fibre. J. Mater. Sci., vol. 2, no. 2, Mar. 1967, pp. 103-111.
9. Stein, Bland A.; and Pride, Richard A.: Effects of 450° F and 600° F Exposures on the Mechanical Properties of Polyimide/Glass-Fiber Honeycomb Sandwiches and Laminated Beams. AIAA Paper No. 67-174, Jan. 1967.
10. Flory, Paul J.: Principles of Polymer Chemistry. Cornell Univ. Press, 1953.
11. Sorenson, Wayne R.; and Campbell, Tod W.: Preparative Methods of Polymer Chemistry. Interscience Publ., Inc., 1961.
12. Bell, Vernon L.: Heteroaromatic Polymers Via Salt Intermediates. J. Polym. Sci., vol. B5, no. 10, 1967, pp. 941-946.
13. Lando, J.; Morosoff, N.; Morawetz, H.; and Post, B.: Single-Crystal Character of Polyoxymethylene Prepared From Single Crystals of Trioxane. J. Polym. Sci., vol. 60, no. 169, July 1962, pp. 824-826.
14. Okamura, S.; Hayashi, K.; and Nishii, M.: Polymer Crystals Obtained by Radiation Polymerization of Trioxane in Solid State. J. Polym. Sci., vol. 60, no. 169, July 1962, pp. 826-829.

15. Okamura, Seizo; Hayashi, Koichiro; and Kitanishi, Yasuhisa: Radiation-Induced Solid-State Polymerization of Ring Compounds. *J. Polym. Sci.*, vol. 58, no. 166, Apr. 1962, pp. 925-953.
16. Kohlschutter, V.; and Tuscher, J. L.: Topochemical Reactions. Formation and Conduct of Cupric Hydroxide. *Z. anorg. allgem. Chem.*, vol. 111, 1920, pp. 193-236.
17. Morawetz, H.; Jakabhazy, S. Z.; Lando, J. B.; and Shafer, J.: Topotactic Reactions in Organic Crystals. *Proc. Nat. Acad. Sci. U.S.*, vol. 49, no. 6, June 1963, pp. 789-793.
18. Cohen, M. D.; and Schmidt, G. M. J.: Topochemistry. I. A Survey. *J. Chem. Soc.*, June 1964, pp. 1996-2000.
19. Nakanishi, Koji: Infrared Absorption Spectroscopy - Practical. Holden-Day, Inc., 1962.
20. Leonard, Nelson J.; and Owens, Frederick H.: Spectral Properties of Medium- and Large-Ring Carbocyclic Compounds:  $\alpha$ -Bromo-Ketones, Enol Acetates and Unsaturated Ketones. *J. American Chem. Soc.*, vol. 80, no. 22, Nov. 20, 1958, pp. 6039-6045.
21. Bellamy, L. J.: The Infra-Red Spectra of Complex Molecules. Second ed., John Wiley & Sons, Inc., 1958.
22. Henry, Norman F. M.; and Lonsdale, Kathleen, eds.: International Tables for X-Ray Crystallography. Volume I - Symmetry Groups. Kynoch Press (Birmingham, England), 1965.
23. Stewart, J. M.; Kruger, G. J.; Ammon, H. L.; Dickinson, C.; and Hall, S. R., eds.: The X-Ray System of Crystallographic Programs for any Computer Having a Pidgin FORTRAN Compiler. Tech. Rep. TR-192, Univ. Maryland Computer Science Center, June 1972. (Available as NASA CR-29908.)
24. Hamilton, Walter C.: On the Treatment of Unobserved Reflexions in the Least-Squares Adjustment of Crystal Structures. *Acta Crystallogr.*, vol. 8, pt. 3, Mar. 1955, pp. 185-186.
25. Azaroff, Leonid V.: Polarization Correction for Crystal-Monochromatized X-Radiation. *Acta Crystallogr.*, vol. 8, pt. 11, Nov. 1955, pp. 701-704.
26. Howells, E. R.; Phillips, D. C.; and Rogers, D.: The Probability Distribution of X-Ray Intensities. II. Experimental Investigation and the X-Ray Detection of Centres of Symmetry. *Acta Crystallogr.*, vol. 3, pt. 3, May 1950, pp. 210-214.
27. Lipson, H.; and Cochran, W.: The Determination of Crystal Structures. G. Bell and Sons, Ltd., 1966.

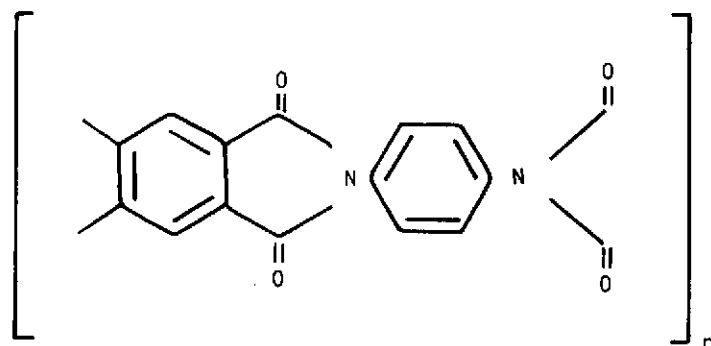
28. Busing, W. R.; Levy, H. A.; and Martin, K. O.: ORFLS, a FORTRAN Crystallographic Least-Squares Program. ORNL-TM-305, U.S. At. Energy Comm., Aug. 1962.
29. Long, Robert Everson: The Crystal and Molecular Structures of 7,7,8,8-Tetracyanoquinodimethane and Cyclopropanecarboxamide, and a Program for Phase Determination. Ph. D. Diss., Univ. of California, 1965.
30. Sayre, D.: The Squaring Method: A New Method for Phase Determination. *Acta Crystallogr.*, vol. 5, pts. 1-3, Jan.-May 1952, pp. 60-65.
31. Karle, J.: Partial Structural Information Combined With the Tangent Formula for Noncentrosymmetric Crystals. *Acta Crystallogr.*, vol. B24, pt. 2, Feb. 15, 1968, pp. 182-186.
32. Karle, Isabella L.; and Karle, J.: Structure of the Chromophore From the Fluorescent Peptide Produced by Iron-Deficient *Azotobacter Vinelandii*. *Acta Crystallogr.*, vol. B27, pt. 10, Oct. 15, 1971, pp. 1891-1898.
33. Karle, Jerome: Translation Functions and Direct Methods. *Acta Crystallogr.*, vol. B28, pt. 3, Mar. 15, 1972, pp. 820-824.
34. Young, Philip Ross: Effluent Analysis of Model Pyrrole Compounds by Gas Chromatography. M.S. Thesis, Virginia Polytech. Inst. & State Univ., May 1971.
35. Barrer, Richard M.: Diffusion in and Through Solids. Cambridge Univ. Press, 1941.
36. Adrova, N. A.; Bessonov, M. I.; Laius, L. A.; and Rudakov, A. P.: Polyimides — A New Class of Thermally Stable Polymers. Technomic Publ. Co., Inc., 1970.
37. Wakelin, James H.; Virgin, Hester S.; and Crystal, Eugene: Development and Comparison of Two X-Ray Methods for Determining the Crystallinity of Cotton Cellulose. *J. Appl. Phys.*, vol. 30, no. 11, Nov. 1959, pp. 1654-1662.
38. Statton, W. O.: An X-Ray Crystallinity Index Method With Application to Poly(Ethylene Terephthalate). *J. Appl. Polym. Sci.*, vol. 7, no. 3, May 1963, pp. 803-814.
39. Bosley, D. E.: X-Ray Determination of Crystallinity in Poly(Ethylene Terephthalate). *J. Appl. Polym. Sci.*, vol. 8, no. 4, July 1964, pp. 1521-1529.



(a) Meta complex.



(b) Para complex.



(c) Polyimide.

Figure 1.- Polymerization reactions. (R denotes an isopropyl functional group.)

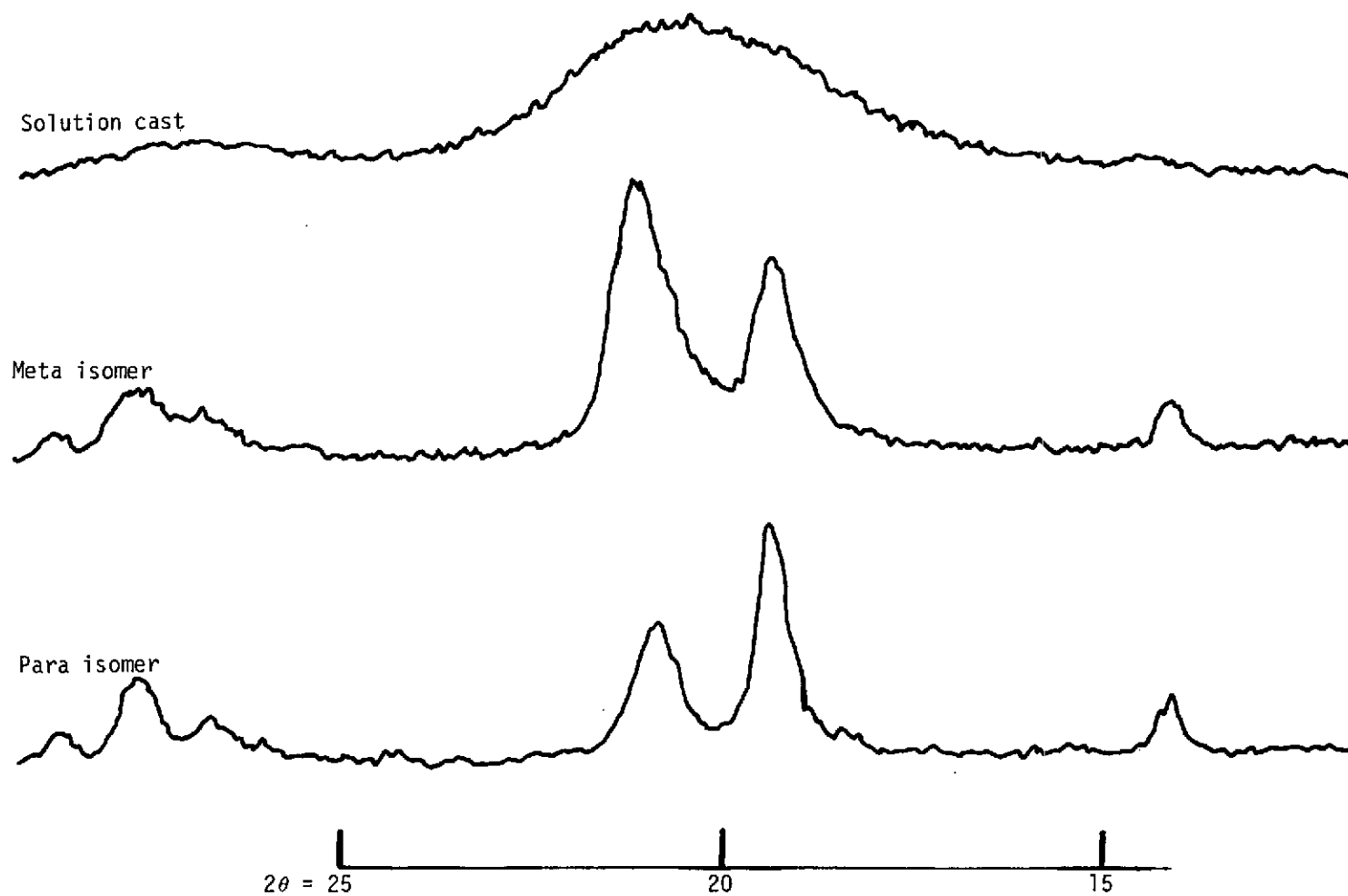


Figure 2.- X-ray powder diffractograms of amorphous solution cast polyimide and crystalline isomeric starting material.

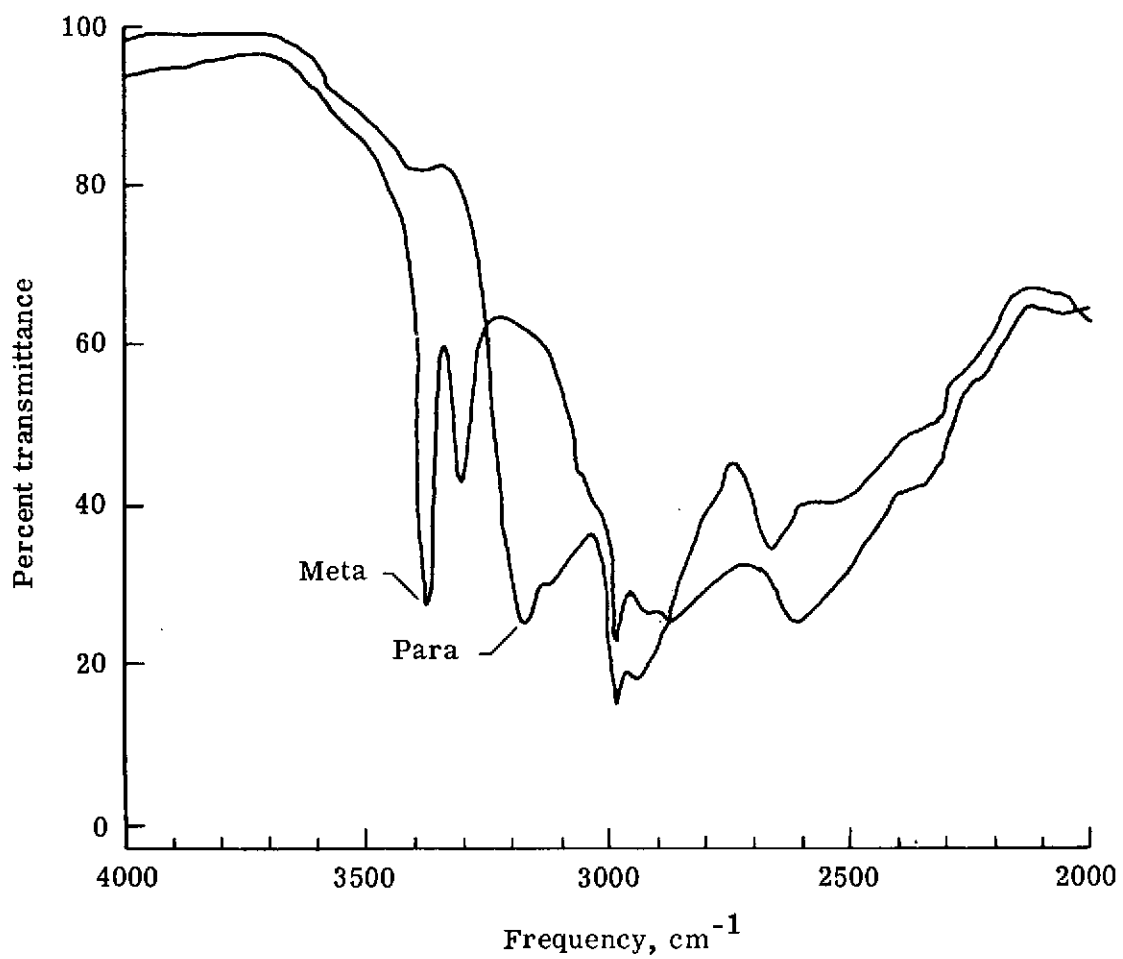


Figure 3.- Infrared spectra of untreated meta and para isomers.

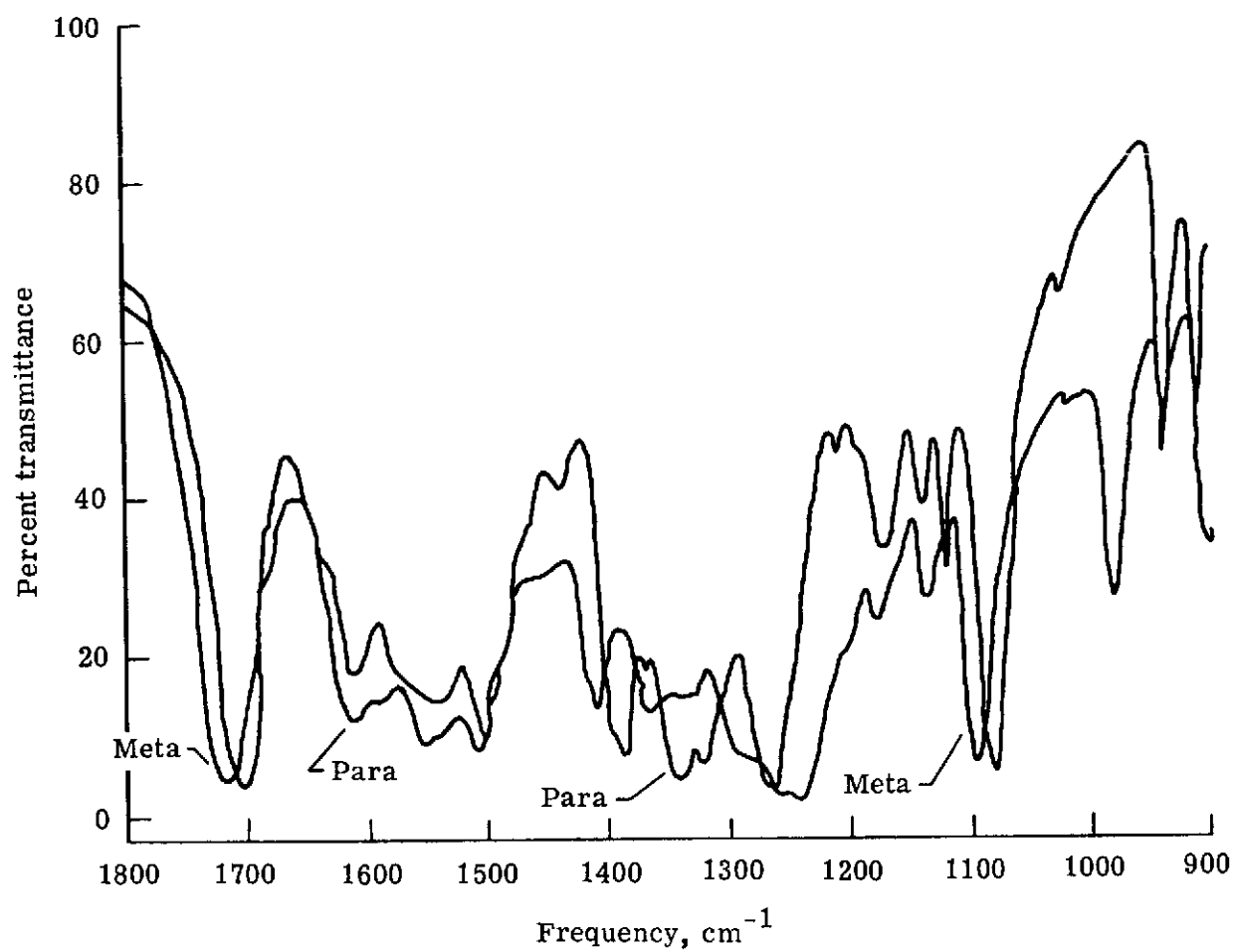


Figure 3.- Concluded.



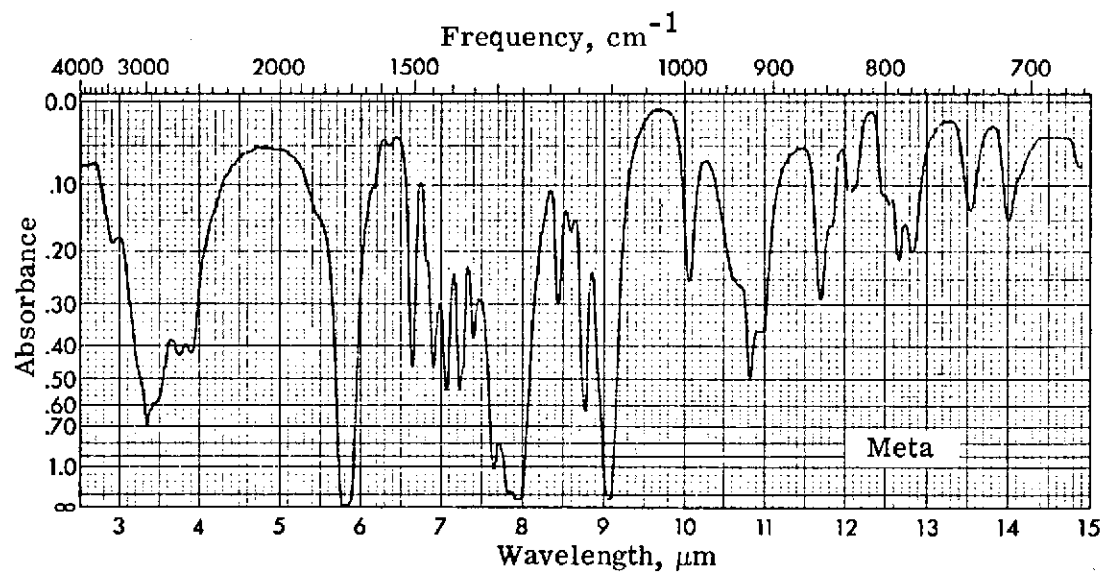
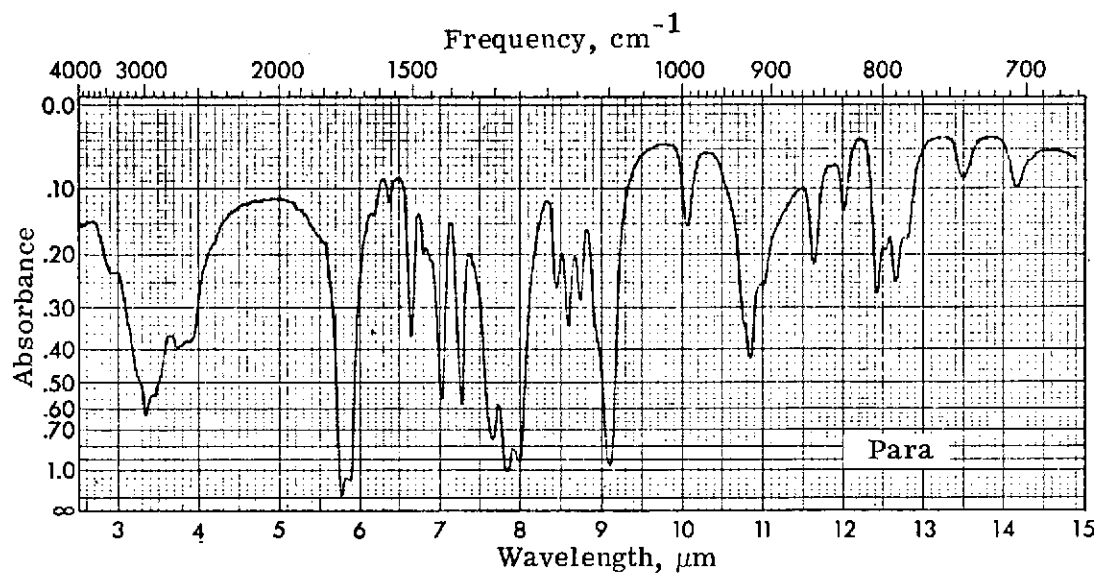


Figure 4.- Infrared spectra of para and meta di-isopropyl pyromellitic acid.

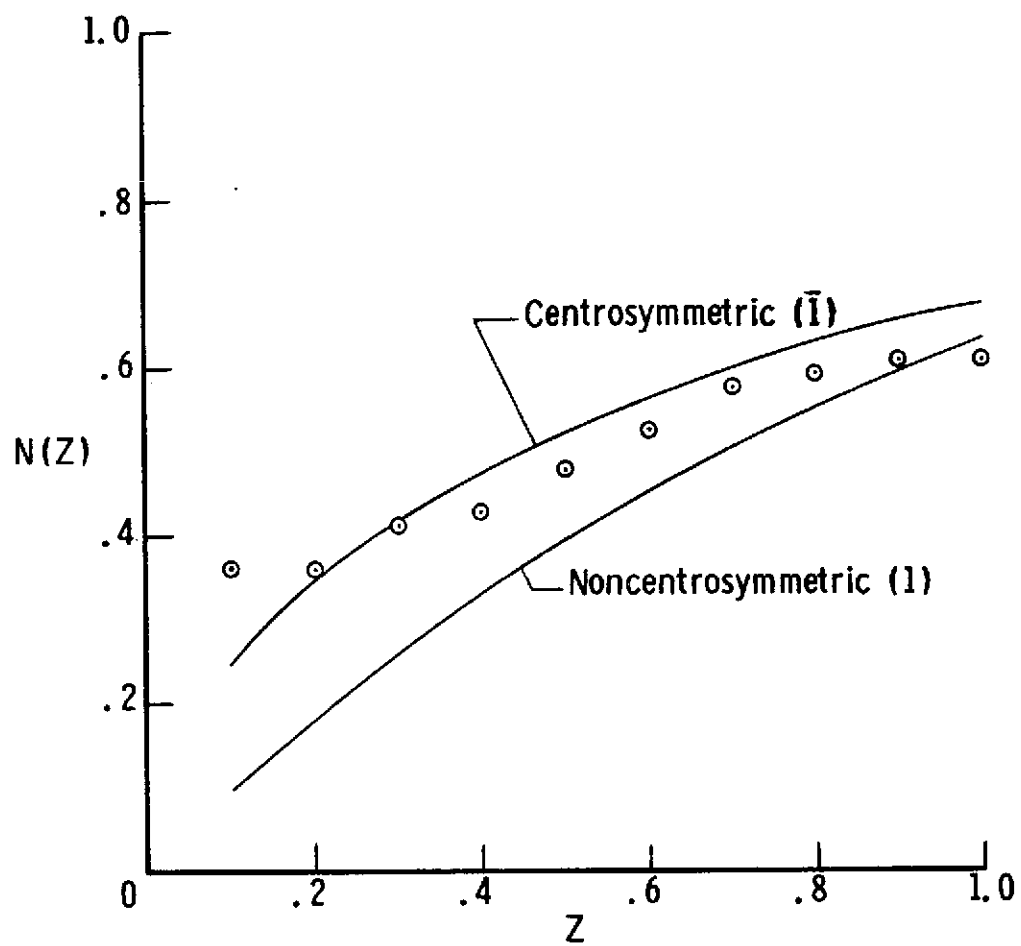


Figure 5.- Zero-moment test.

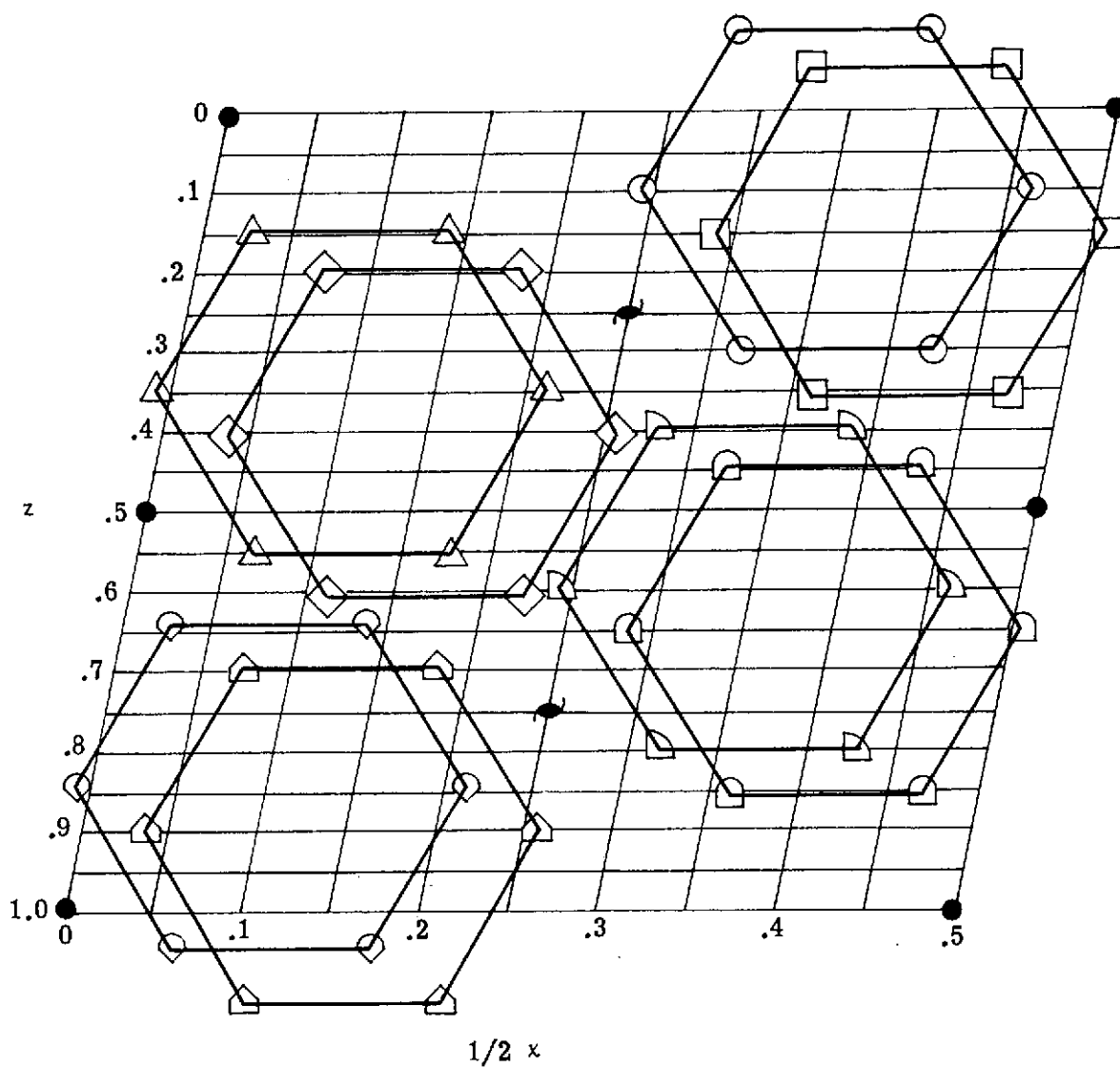


Figure 6.- Minimum residual rings in  $ac$  plane.

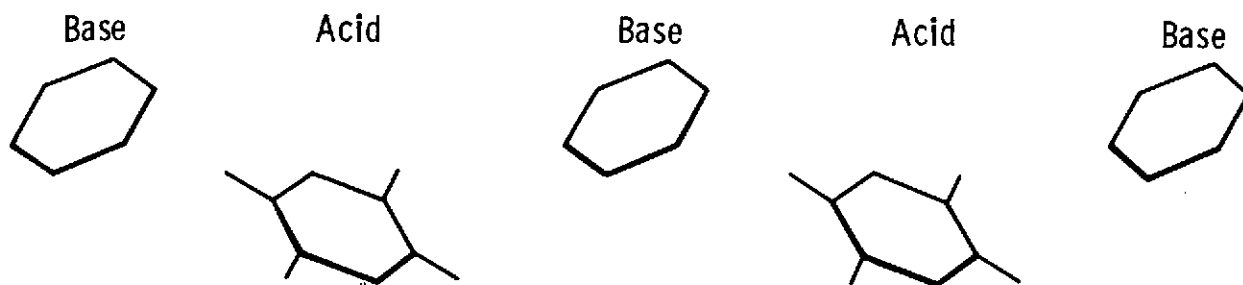
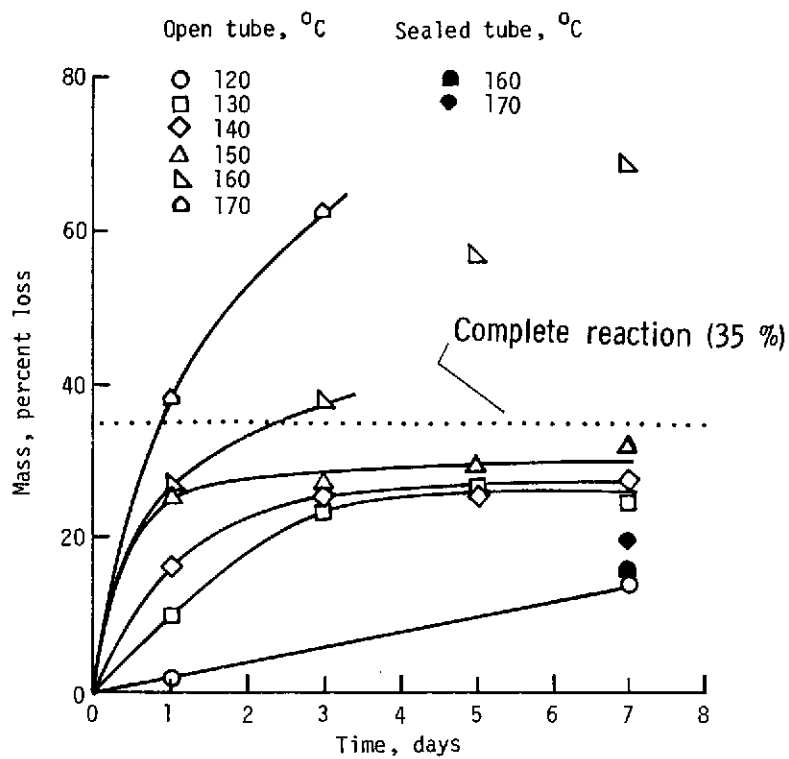
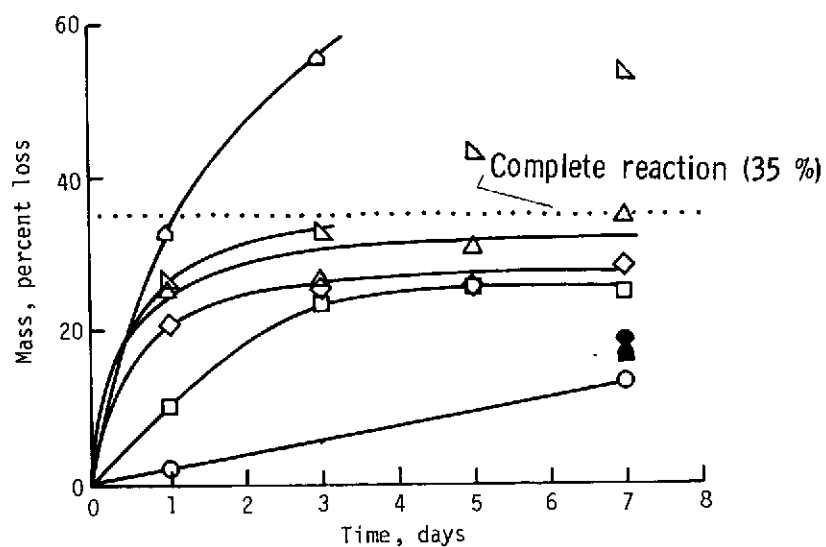


Figure 7.- Representation of molecular orientation of acid and base parts of meta precursor.



(a) Para isomer.



(b) Meta isomer.

Figure 8.- Percent mass loss as a function of time for isothermal annealing.

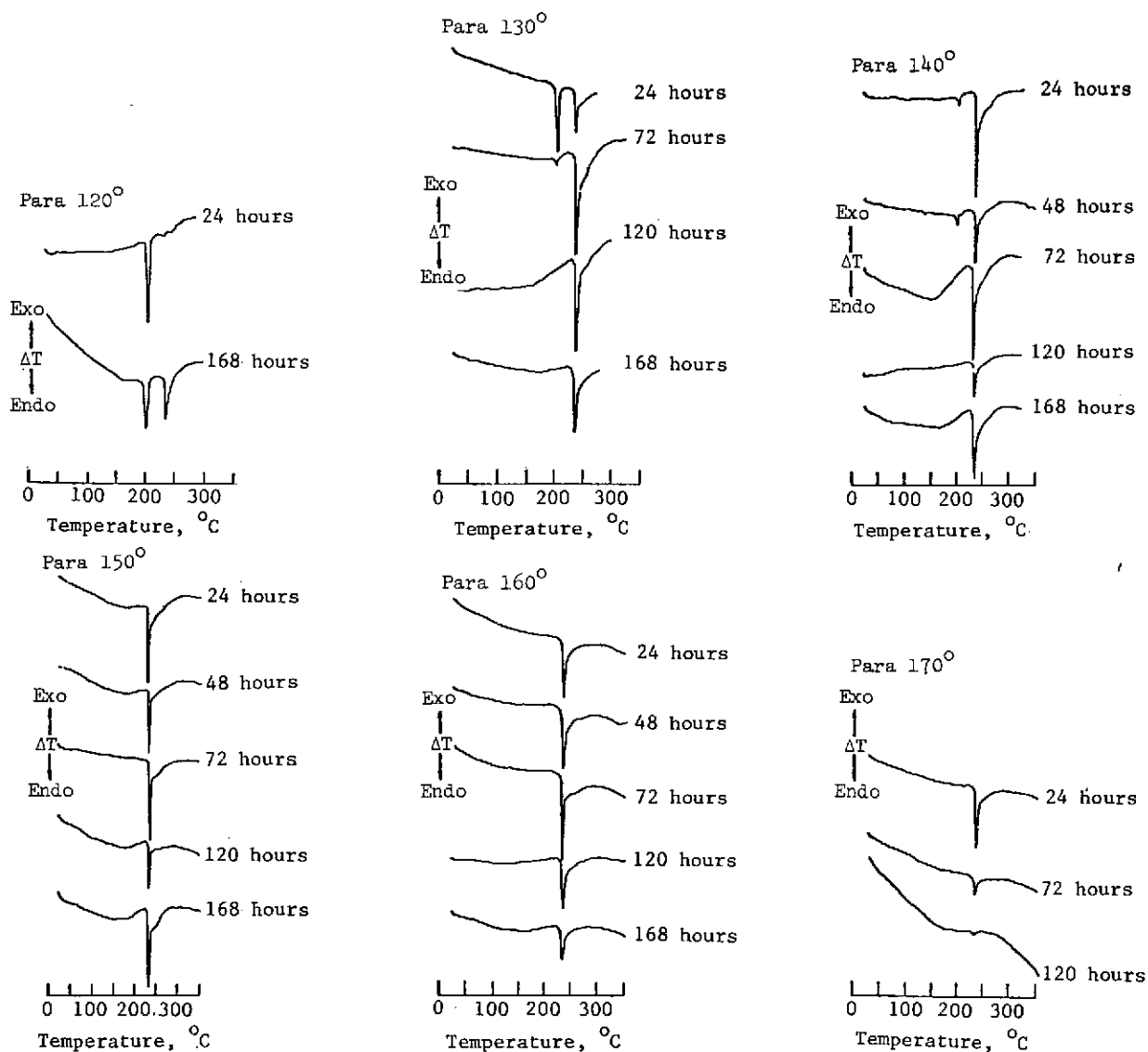


Figure 9.- DTA thermograms of para open tube specimens annealed at specified temperatures. Exo denotes exothermic transition and Endo denotes endothermic transition.

ORIGINAL PAGE IS  
OF POOR QUALITY

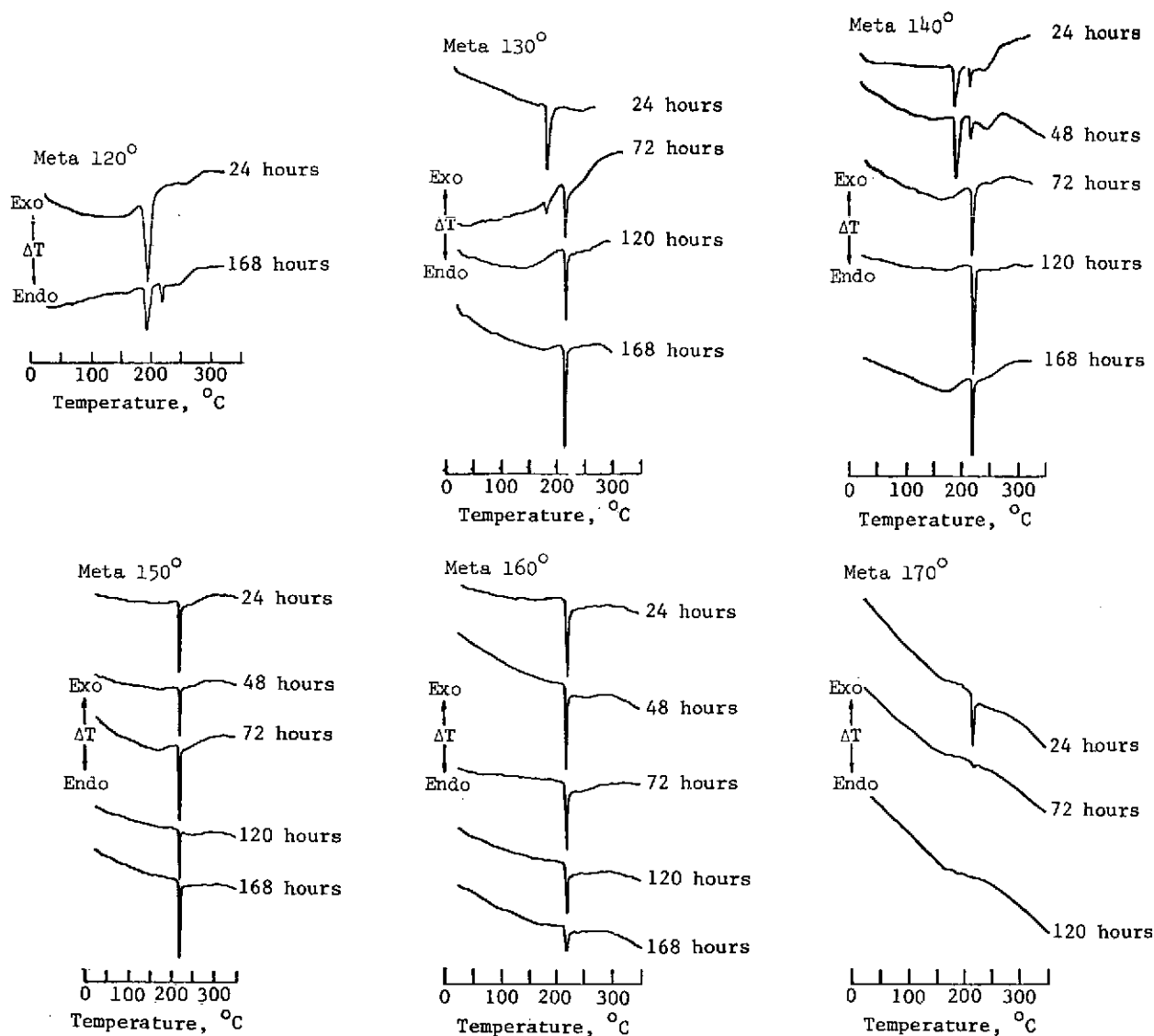


Figure 10.- DTA thermograms of meta open tube specimens annealed at specified temperatures. Exo denotes exothermic transition and Endo denotes endothermic transition.

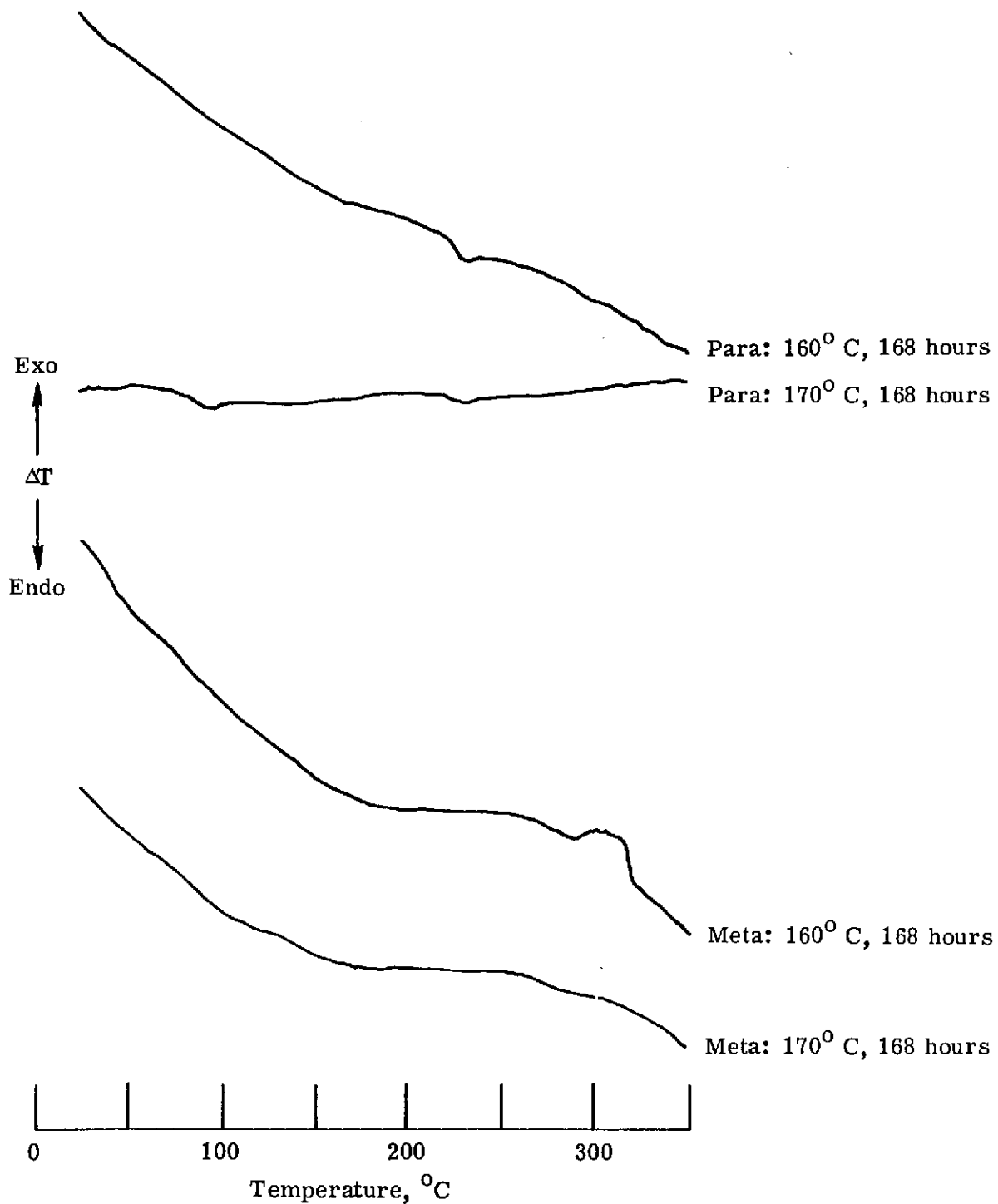


Figure 11.- DTA thermograms of para and meta sealed tube specimens.  
Exo denotes exothermic transition and Endo denotes endothermic transition.

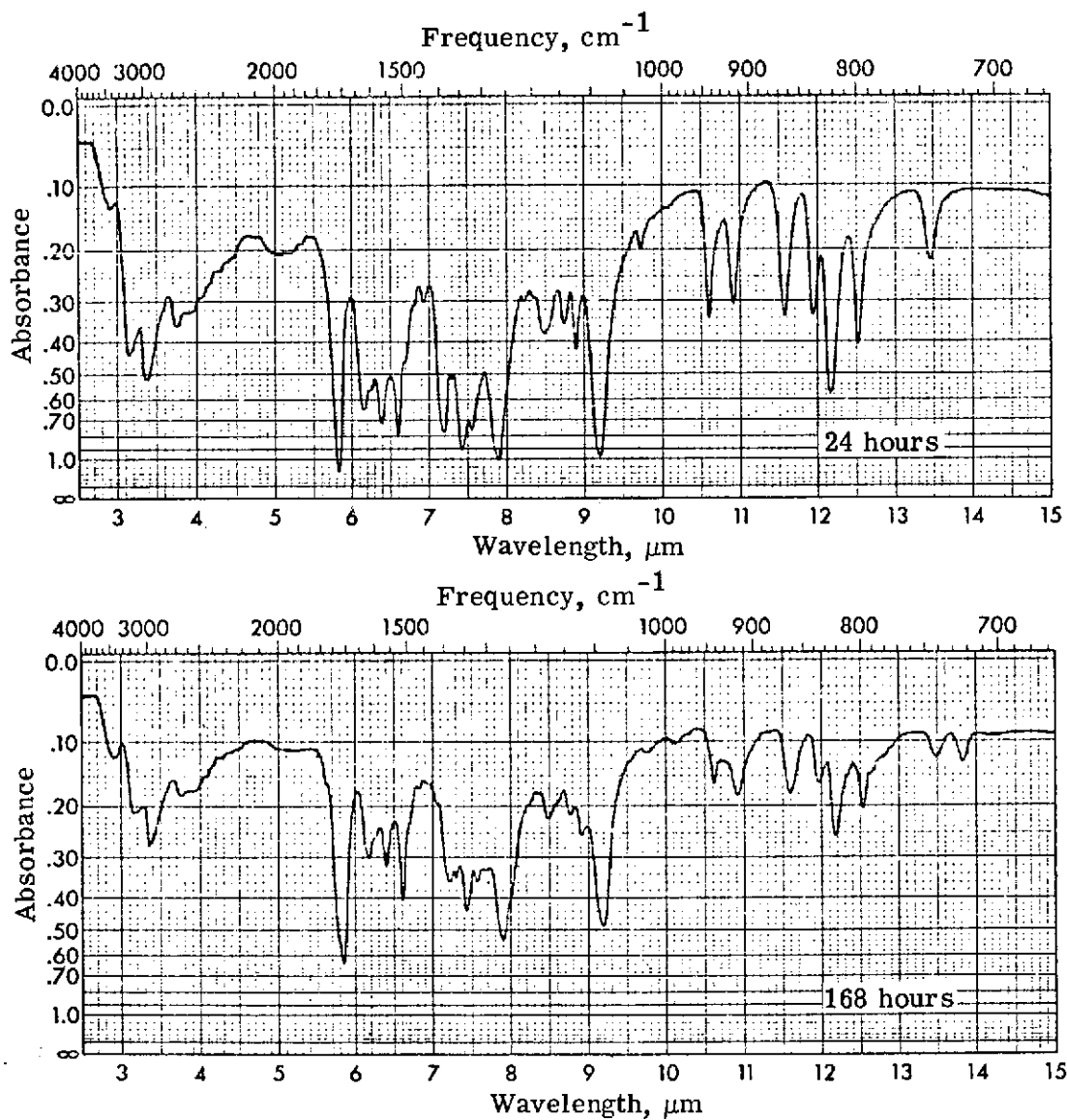


Figure 12.- Infrared spectra of para open tube specimens annealed at 120° C.

ORIGINAL PAGE IS  
OF POOR QUALITY



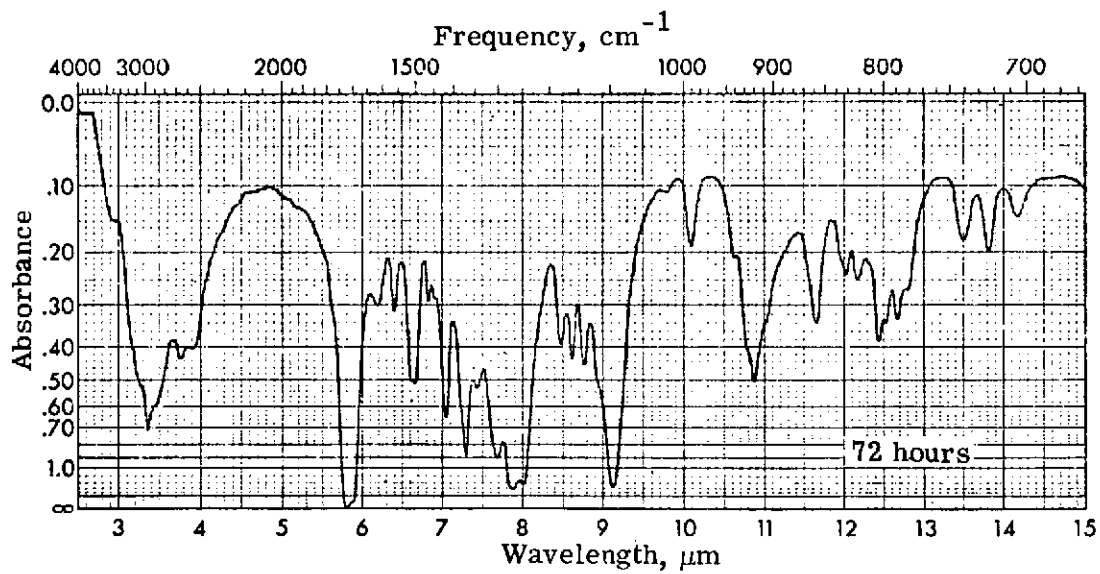
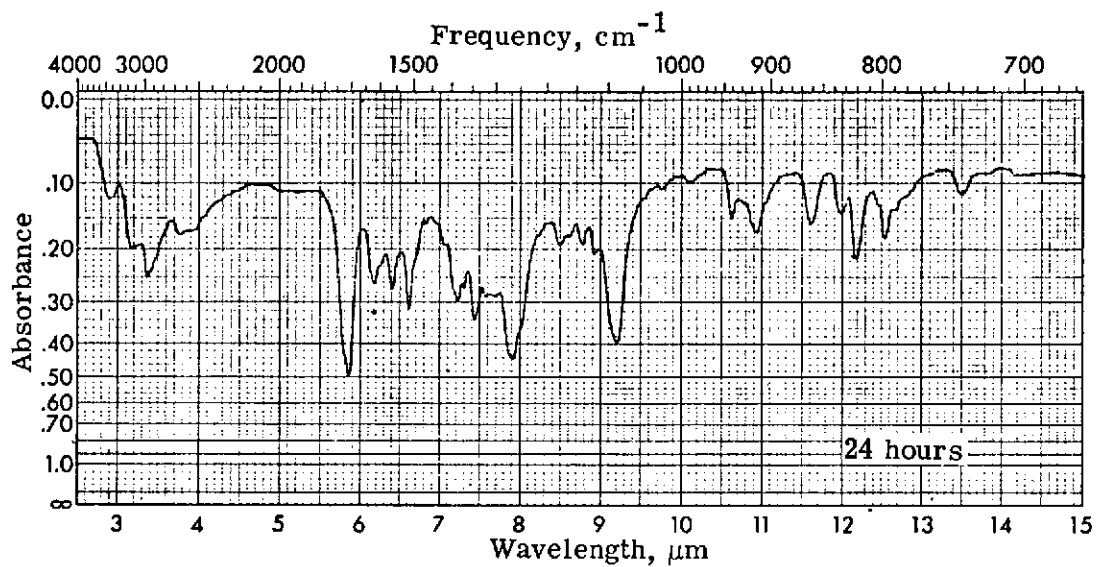


Figure 13.- Infrared spectra of para open tube specimens annealed at  $130^{\circ}\text{C}$ .

ORIGINAL PAGE IS  
OF POOR QUALITY

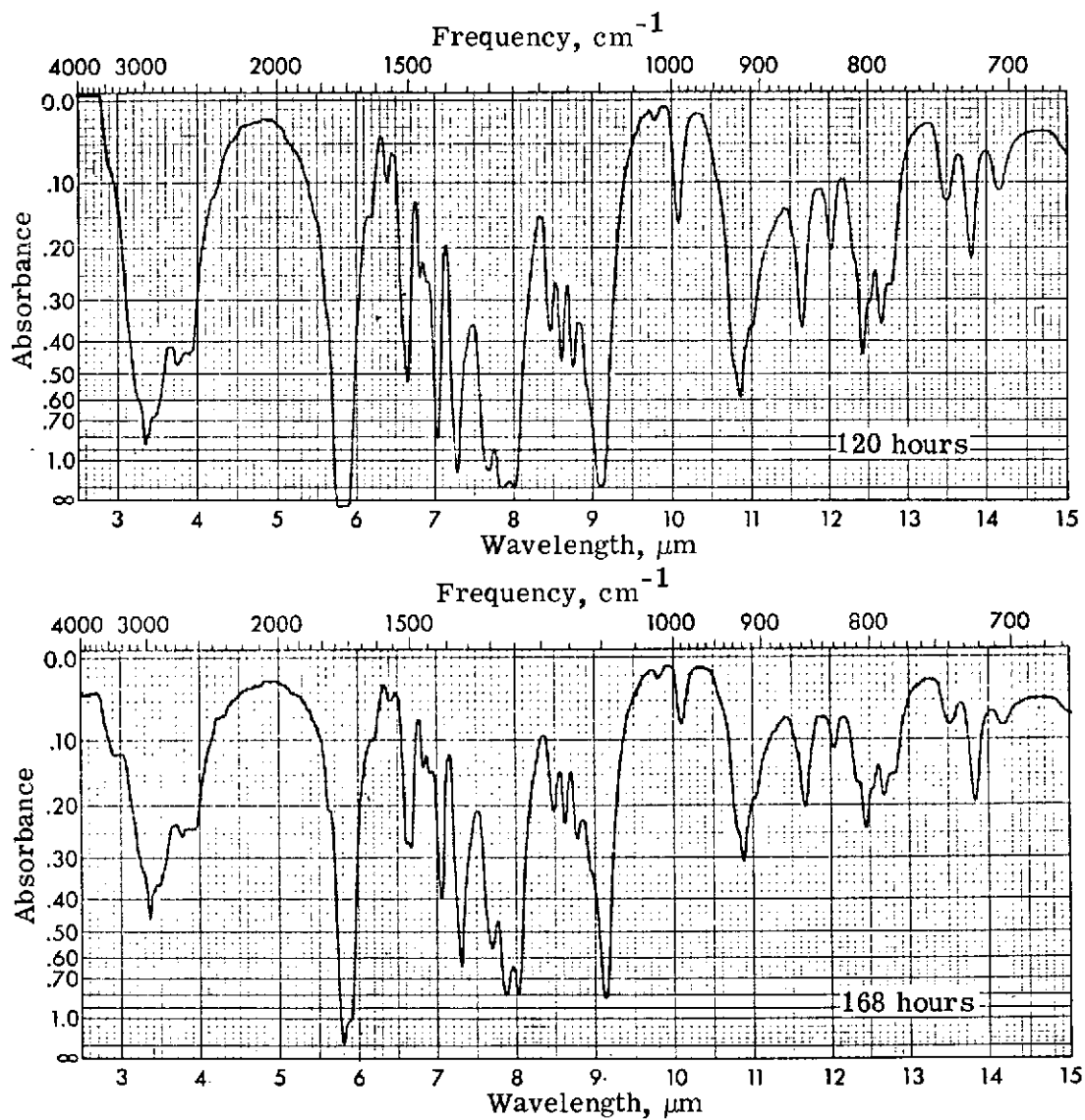


Figure 13.- Concluded.

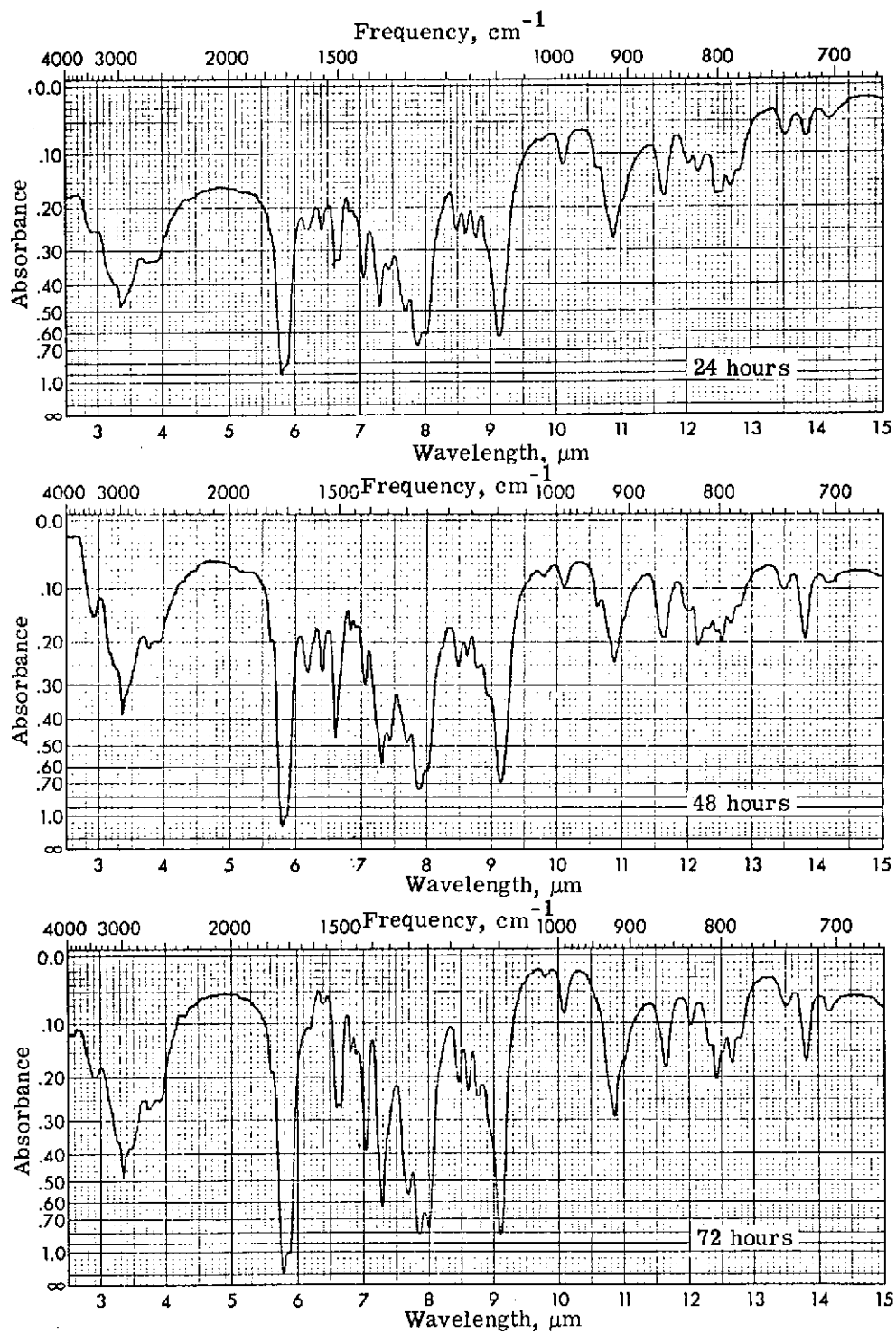


Figure 14.- Infrared spectra of para open tube specimens annealed at  $140^{\circ}\text{C}$ .

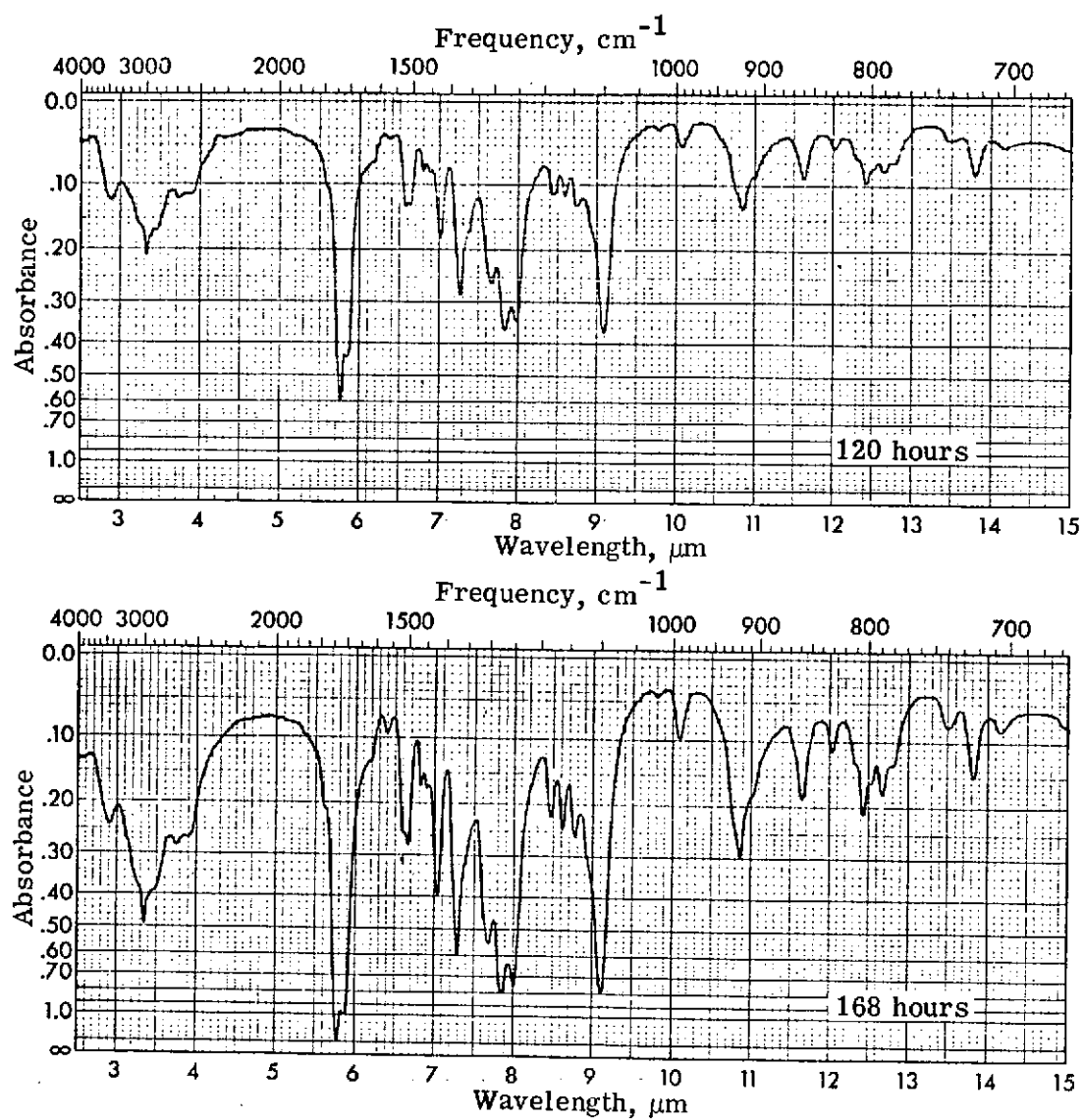


Figure 14.- Concluded.

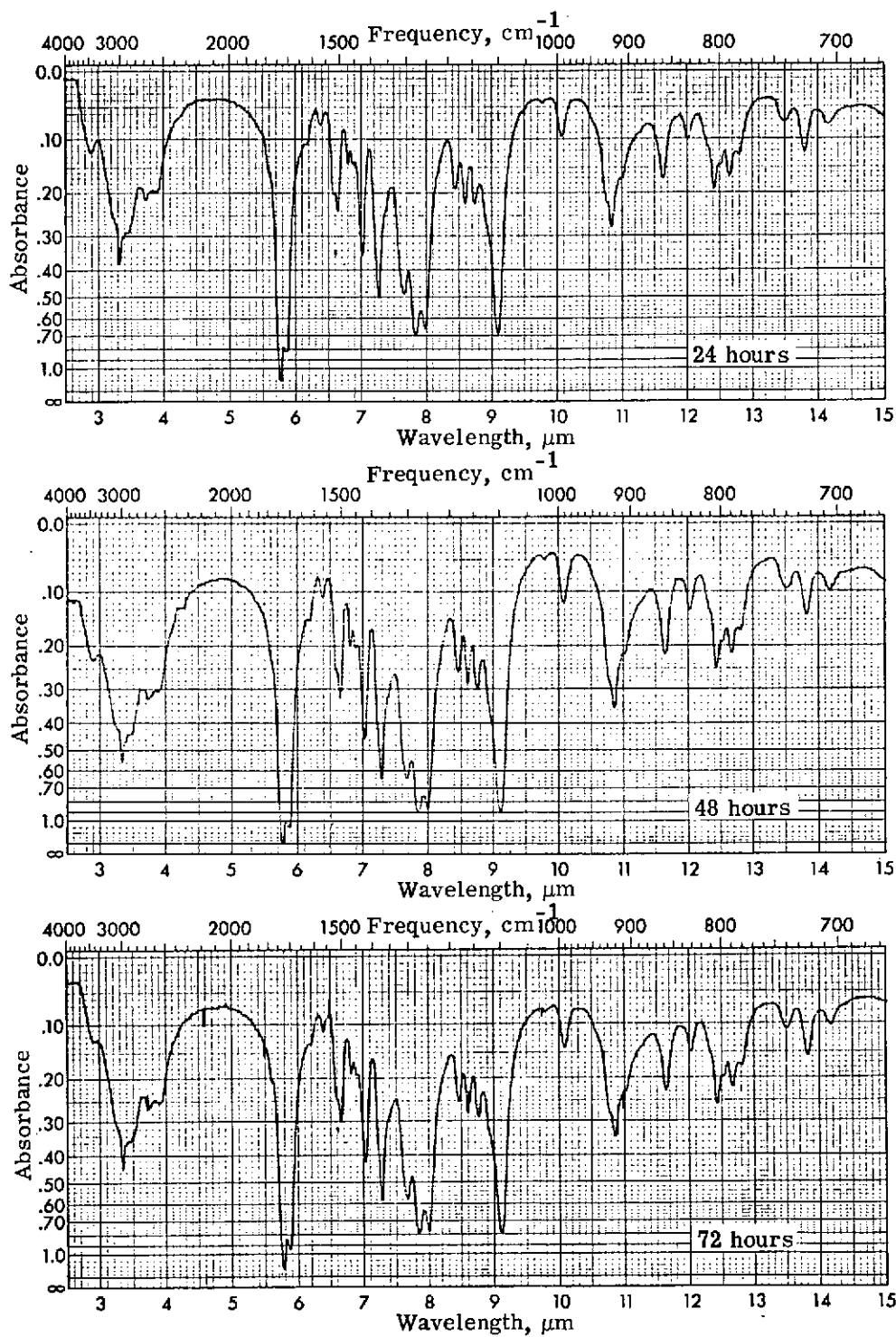


Figure 15.- Infrared spectra of para open tube specimens annealed at  $150^\circ\text{C}$ .

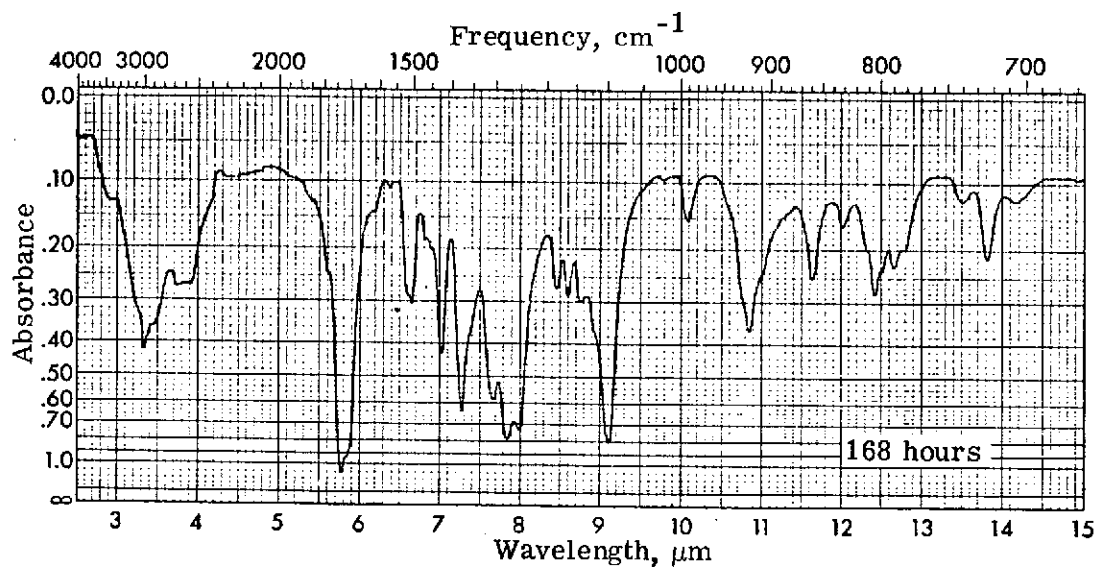
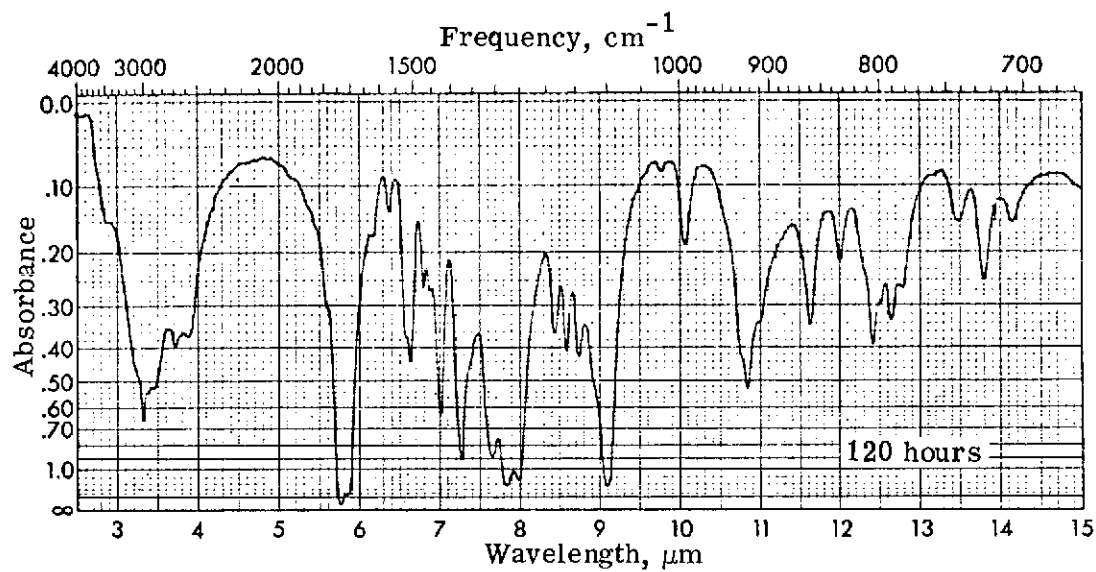


Figure 15.- Concluded.

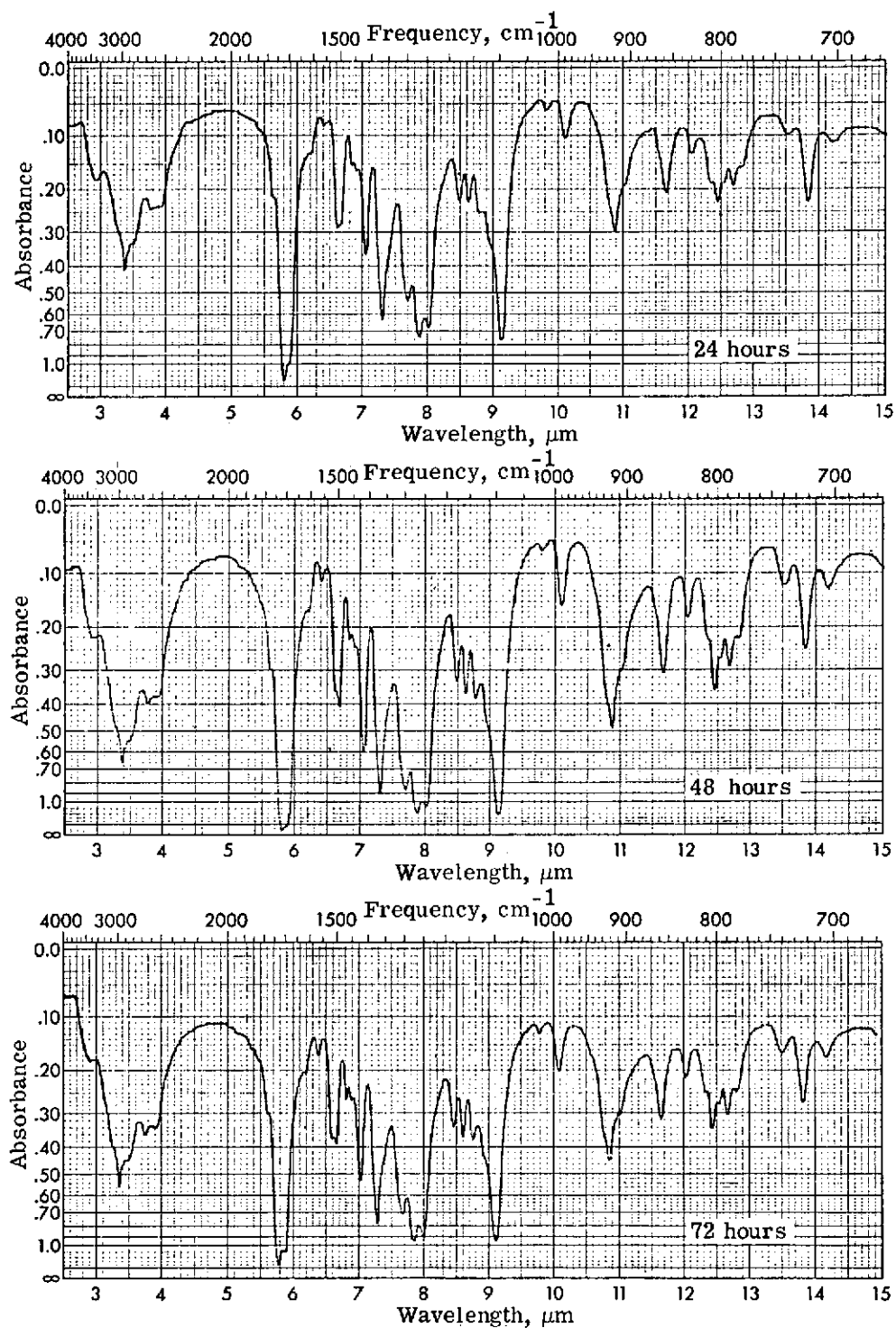


Figure 16.- Infrared spectra of para open tube specimens annealed at  $160^{\circ}\text{C}$ .

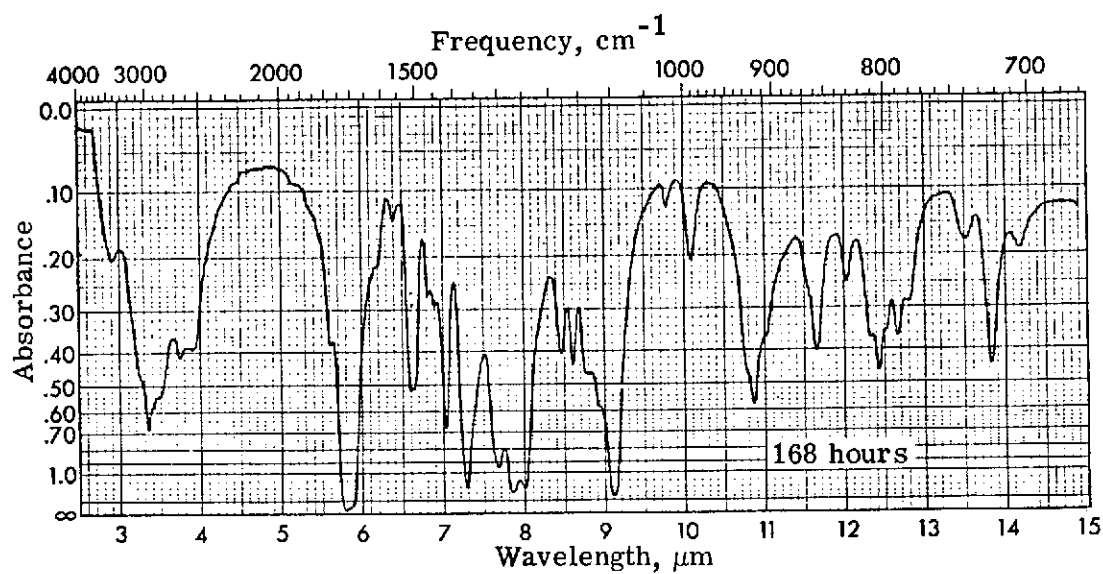
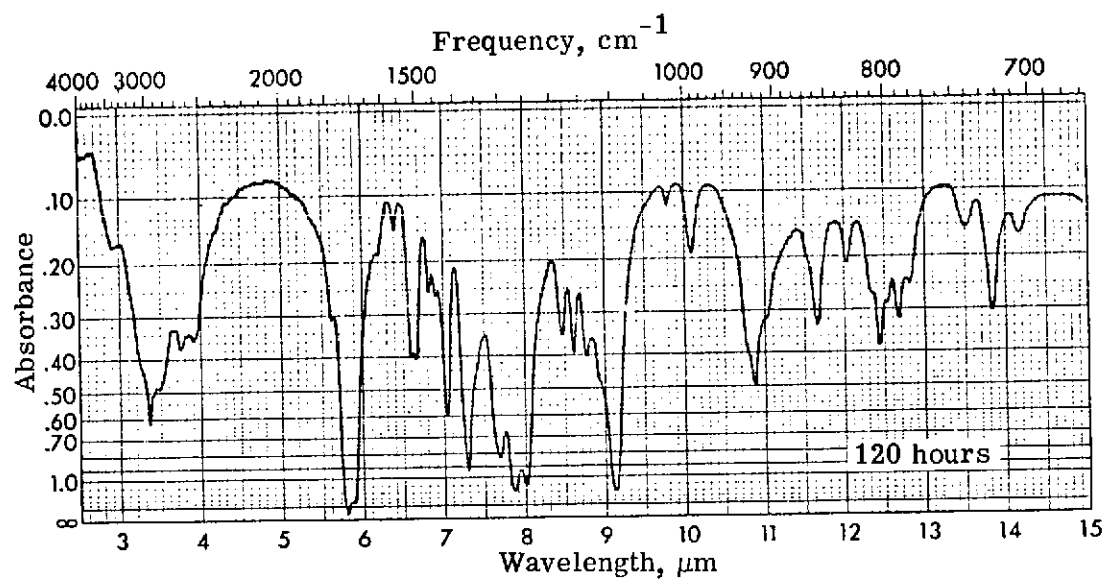


Figure 16.- Concluded.



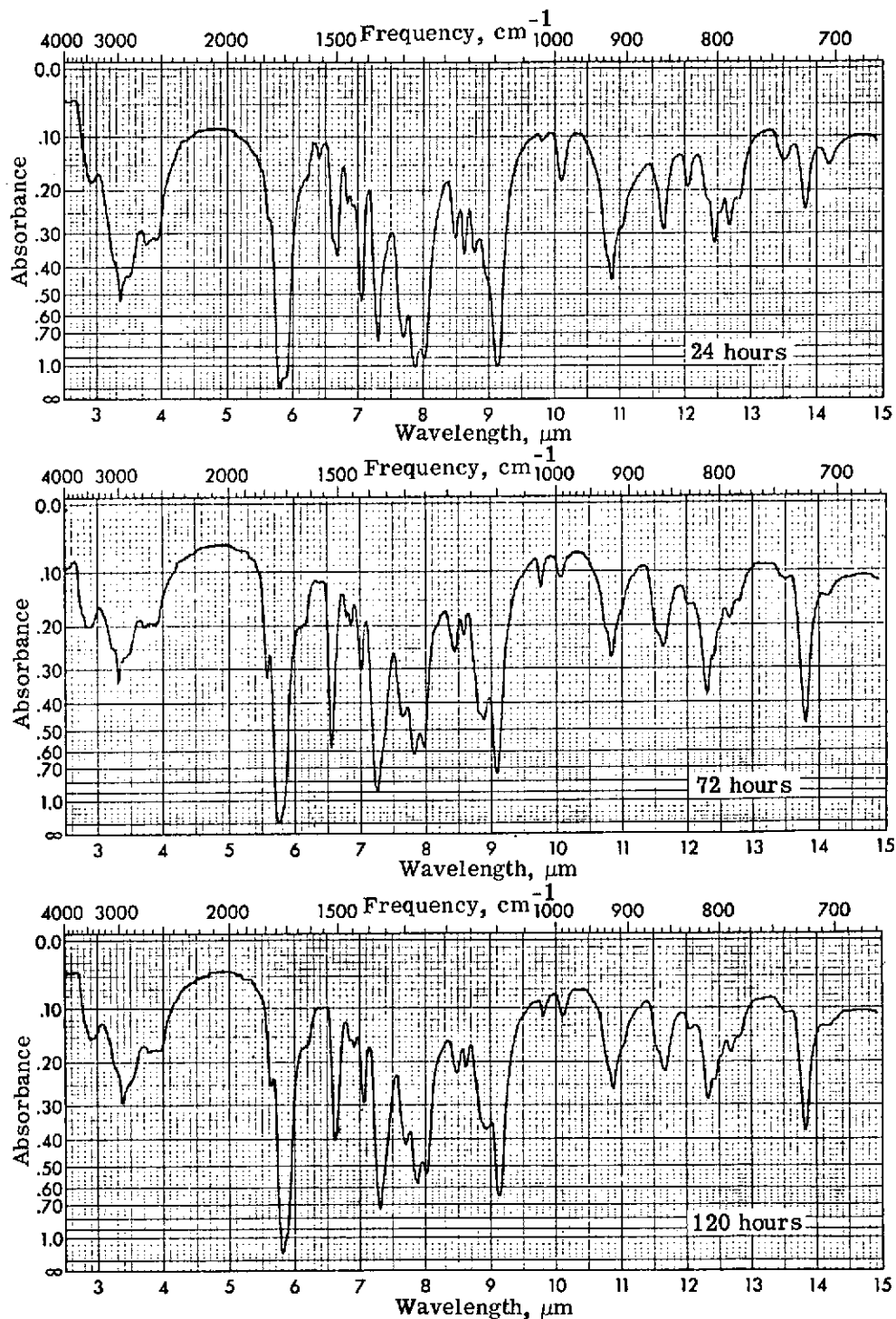


Figure 17.- Infrared spectra of para open tube specimens annealed at 170° C.

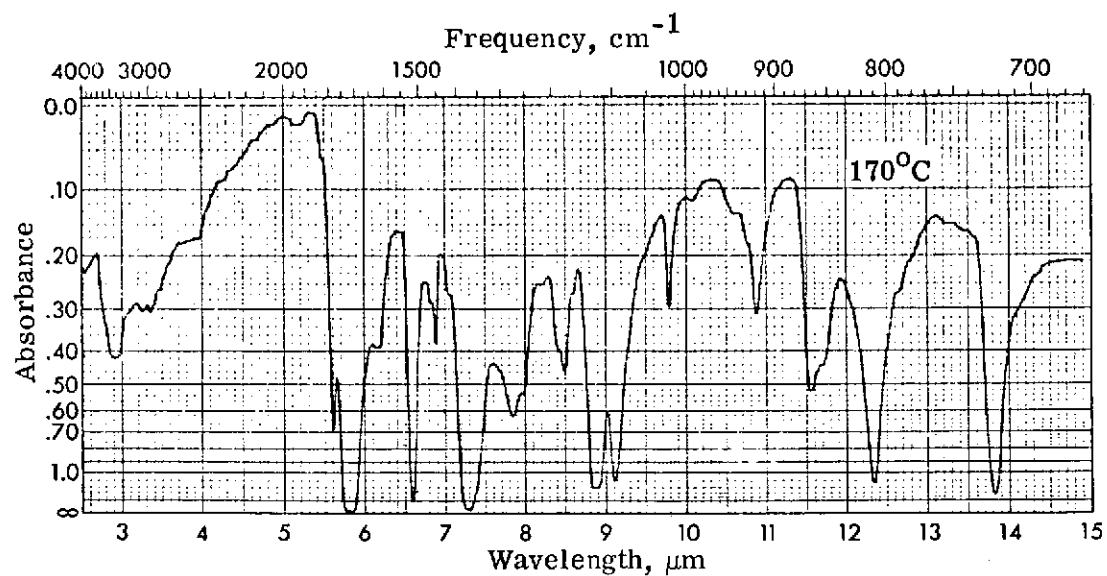
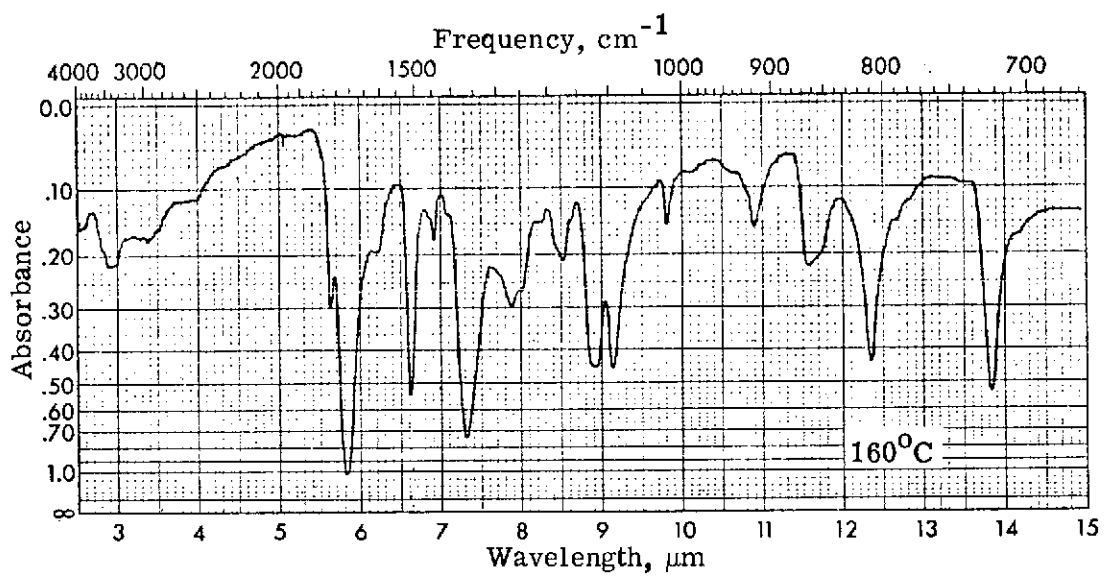


Figure 18.- Infrared spectra of para sealed tube specimens annealed for 168 hours.

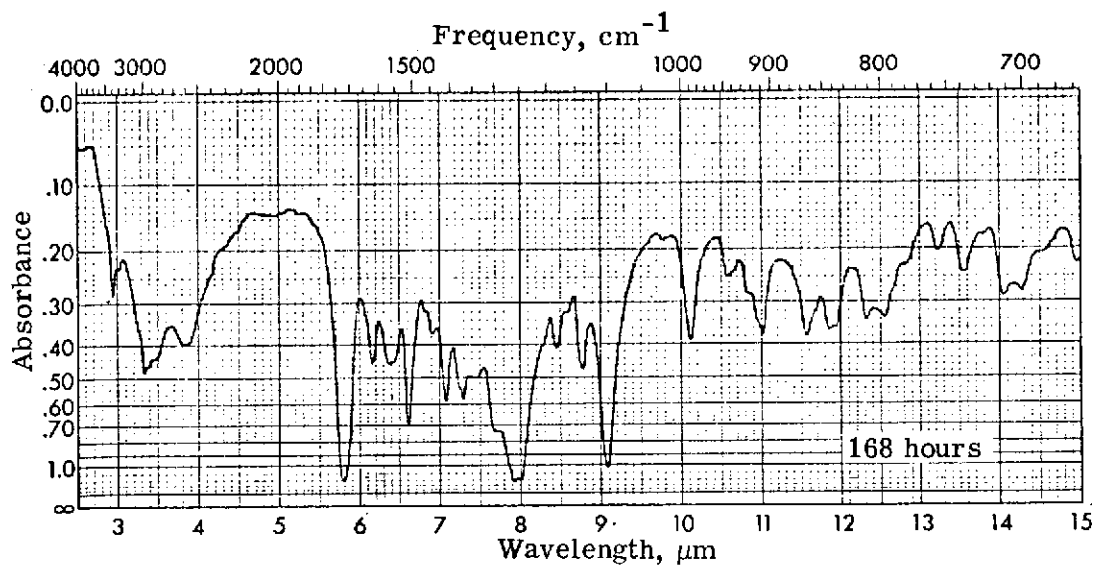
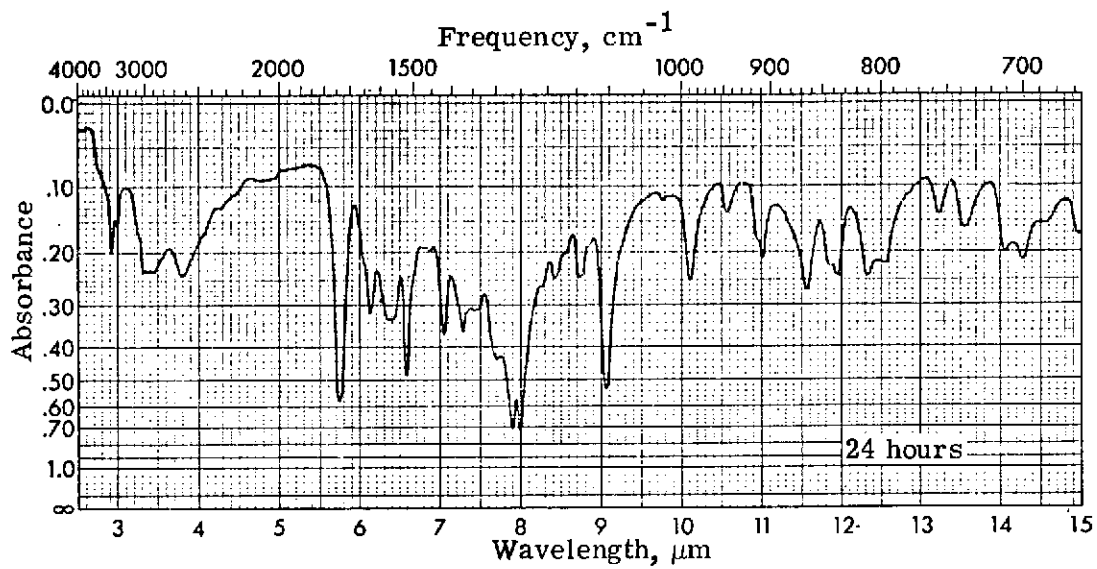


Figure 19.- Infrared spectra of meta open tube specimens annealed at 120° C.

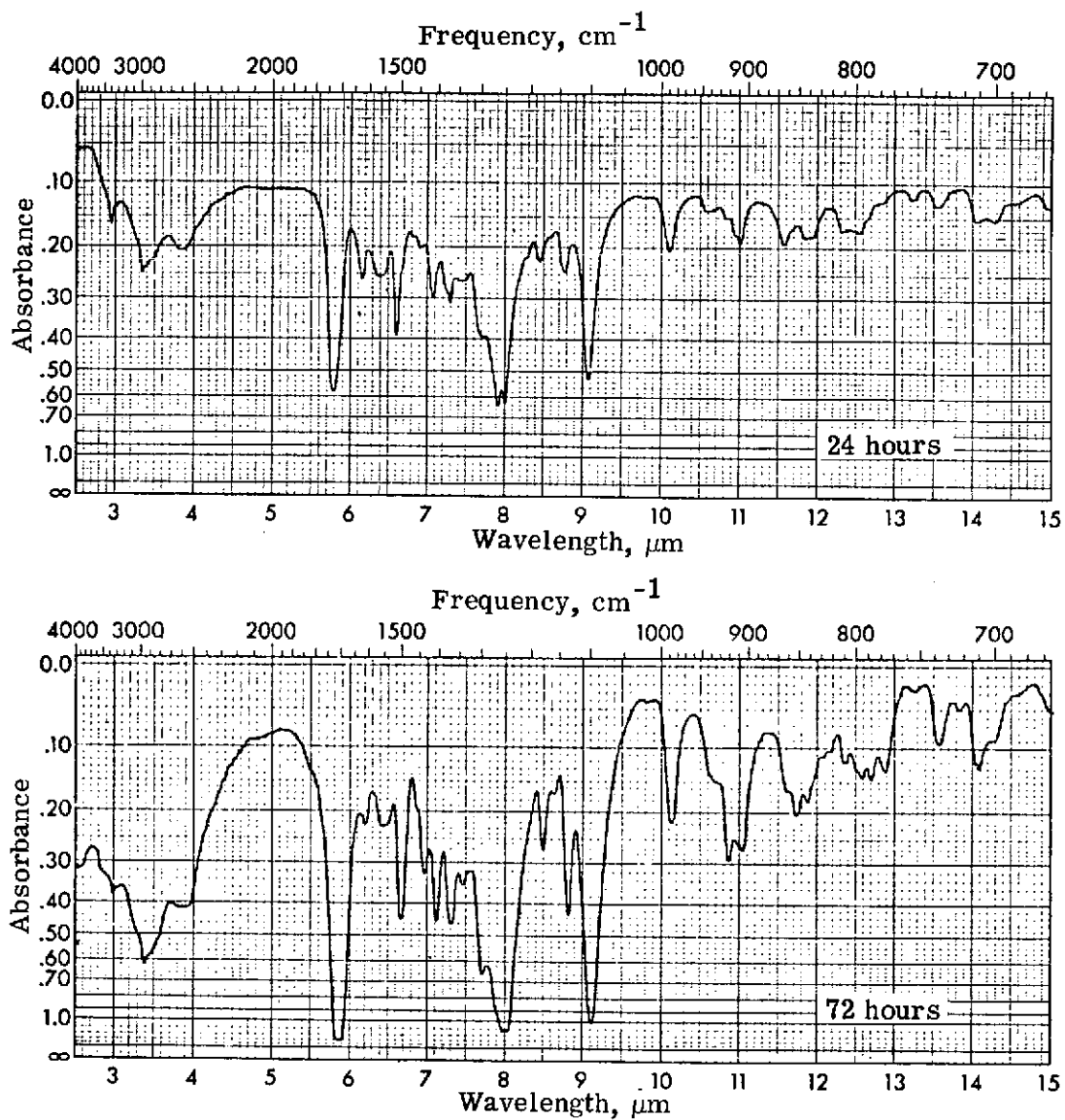


Figure 20. - Infrared spectra of meta open tube specimens annealed at 130° C.

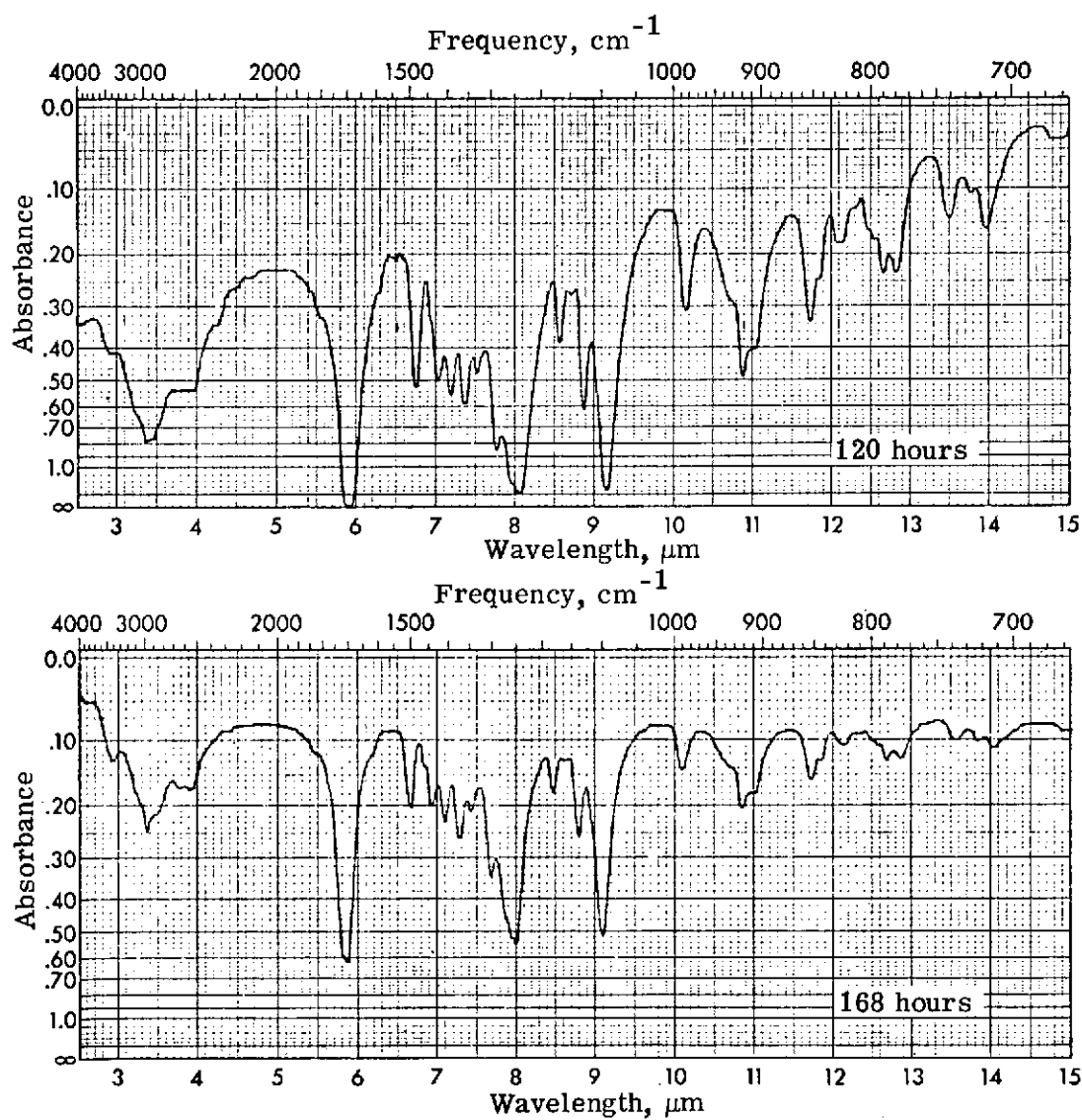


Figure 20.- Concluded.

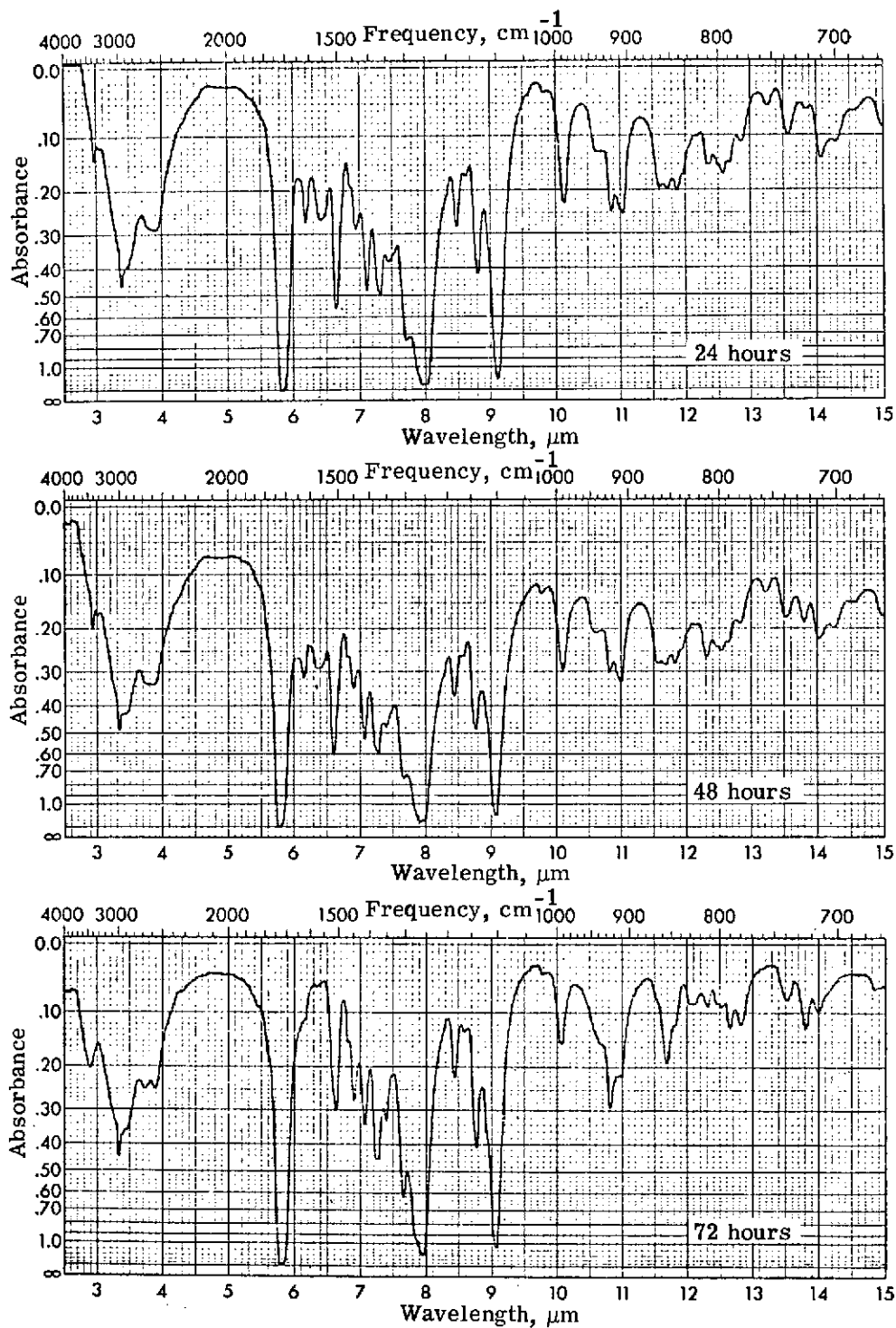


Figure 21.- Infrared spectra of meta open tube specimens annealed at  $140^{\circ}\text{C}$ .

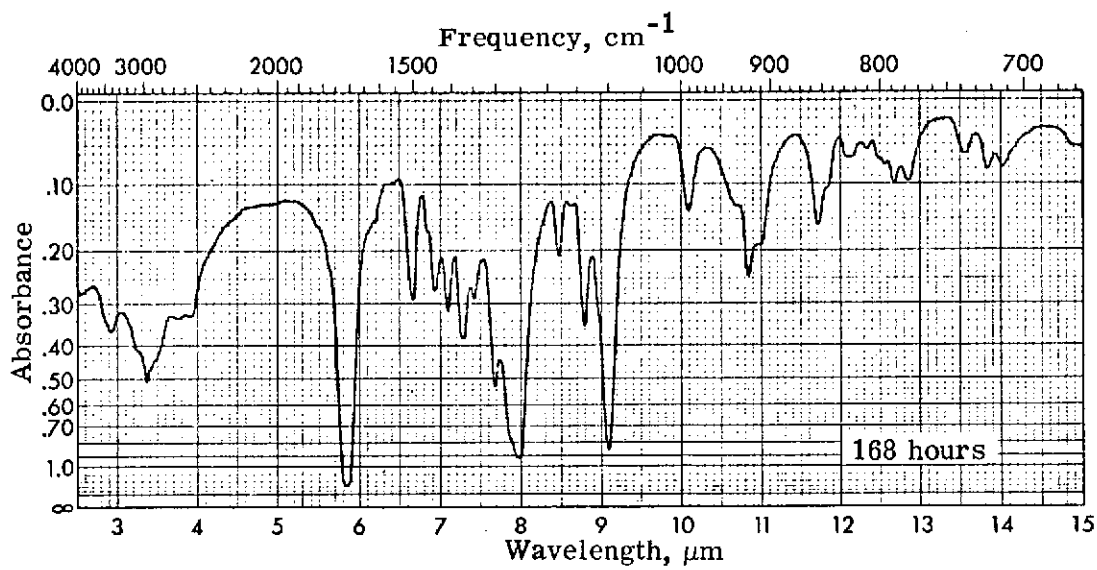
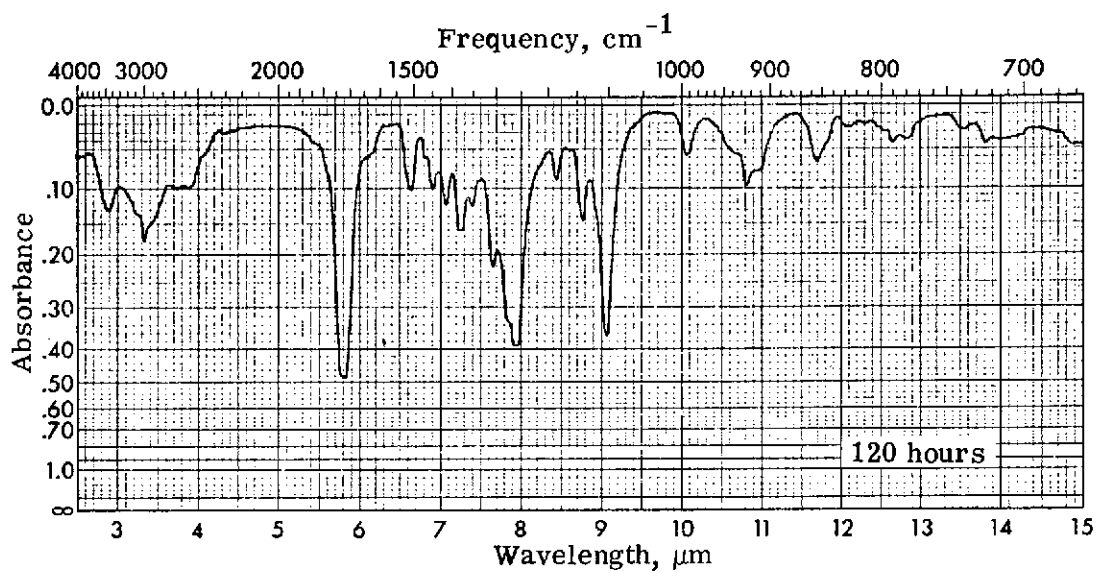


Figure 21.- Concluded.

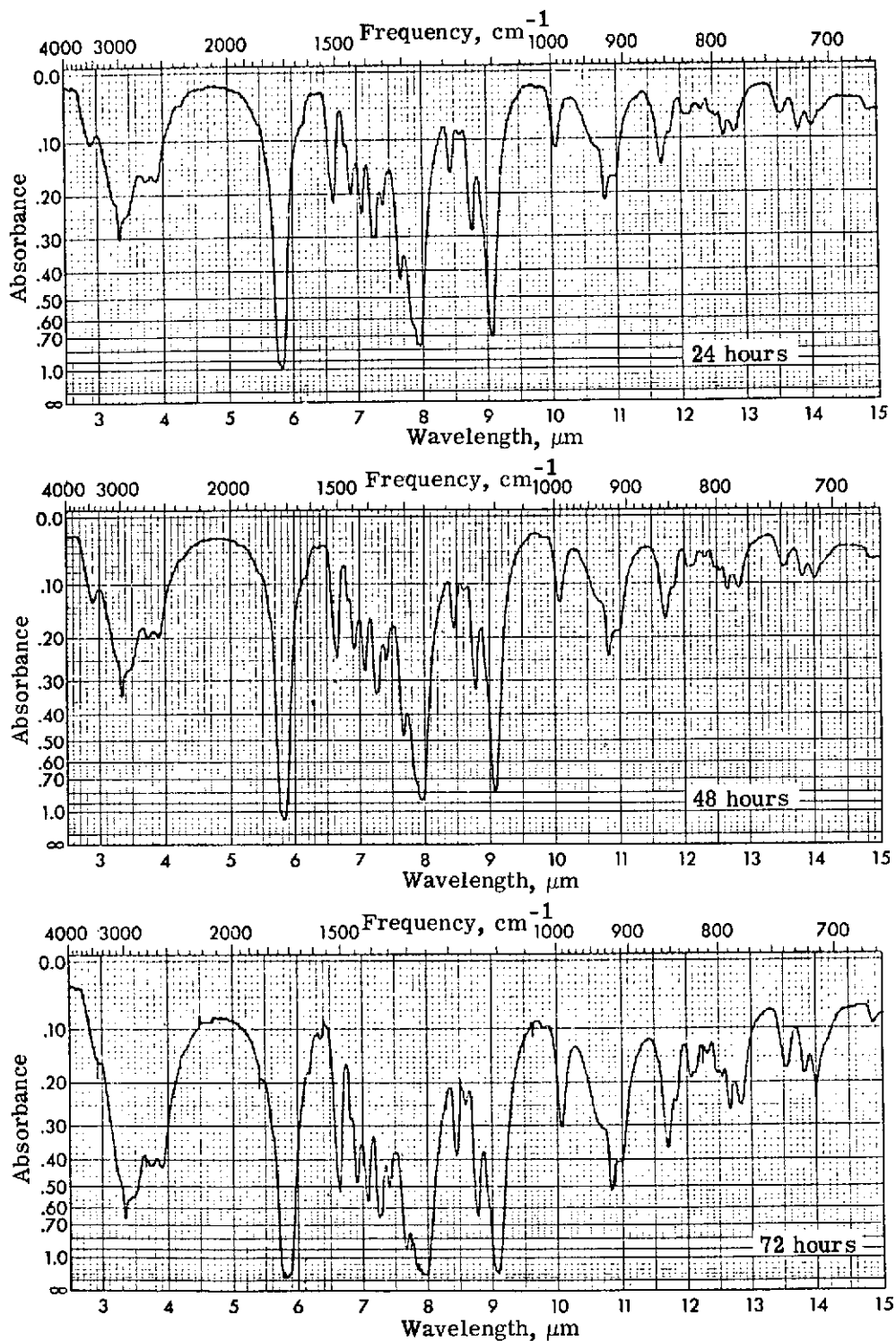


Figure 22.- Infrared spectra of meta open tube specimens annealed at 150° C.



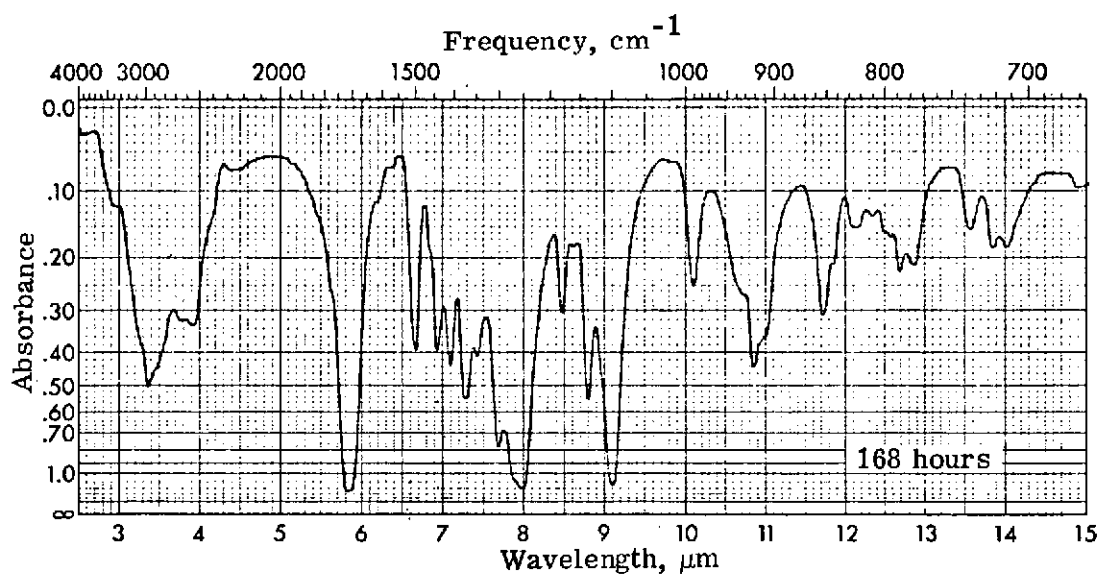
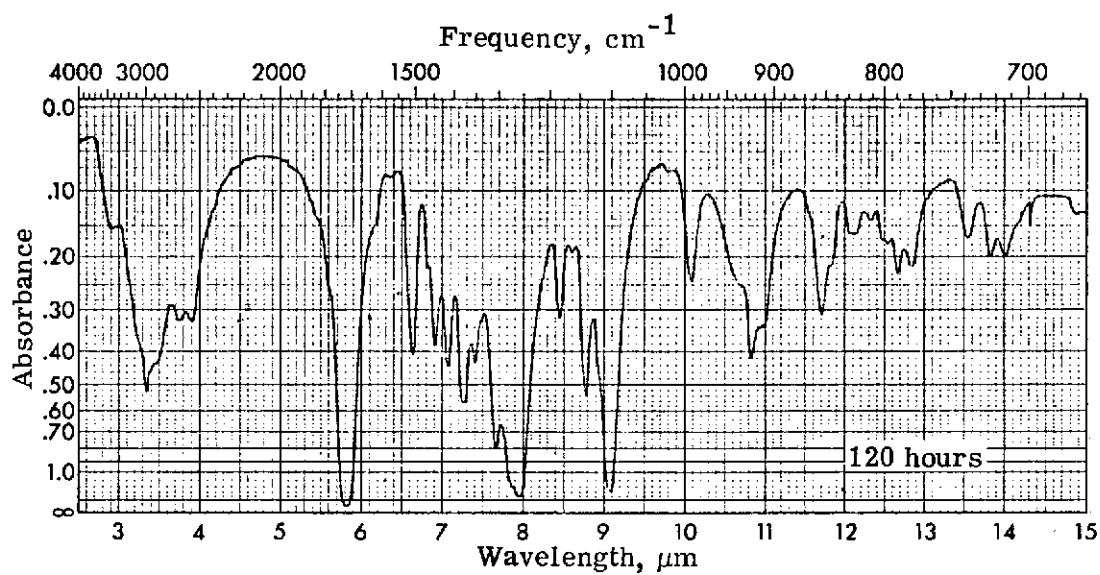


Figure 22.- Concluded.

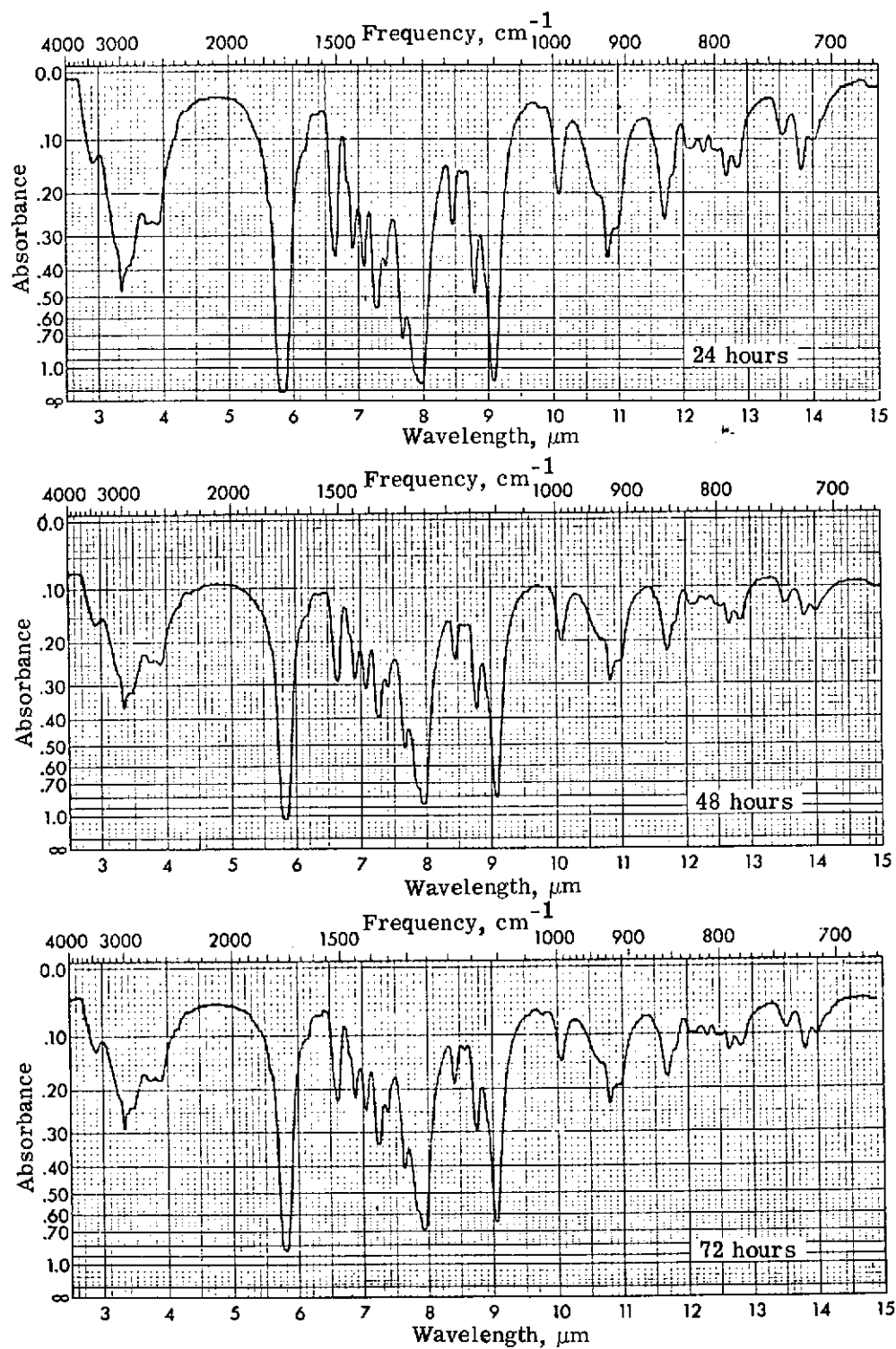


Figure 23.- Infrared spectra of meta open tube specimens annealed at 160° C.

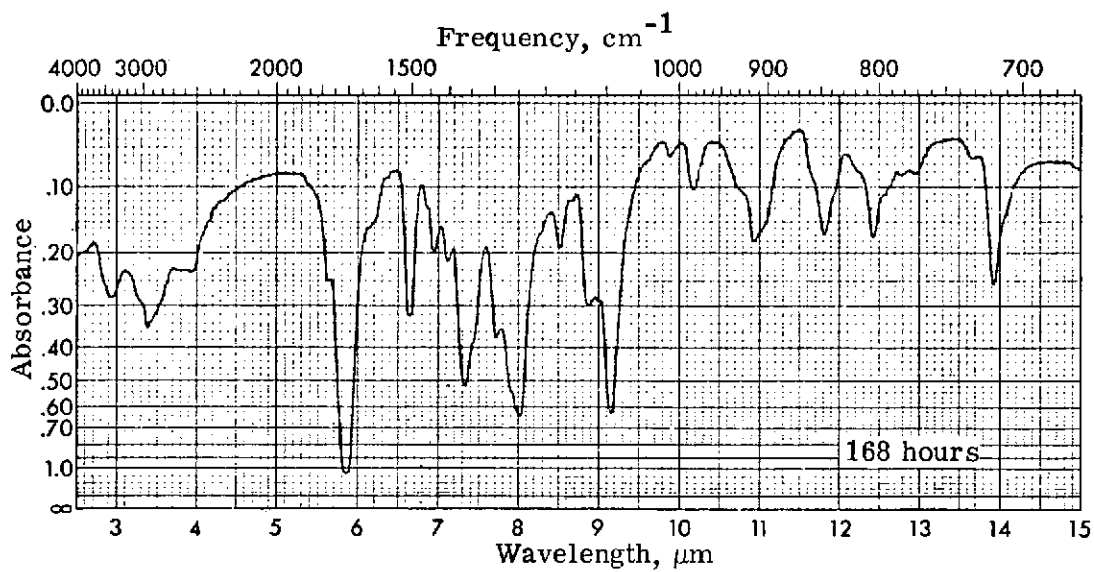
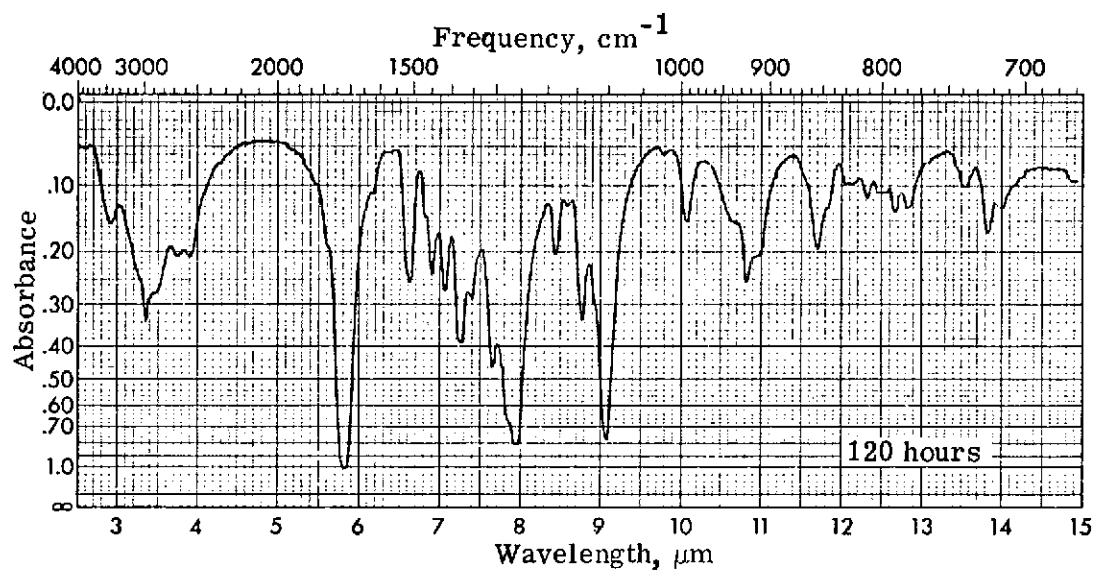


Figure 23.- Concluded.

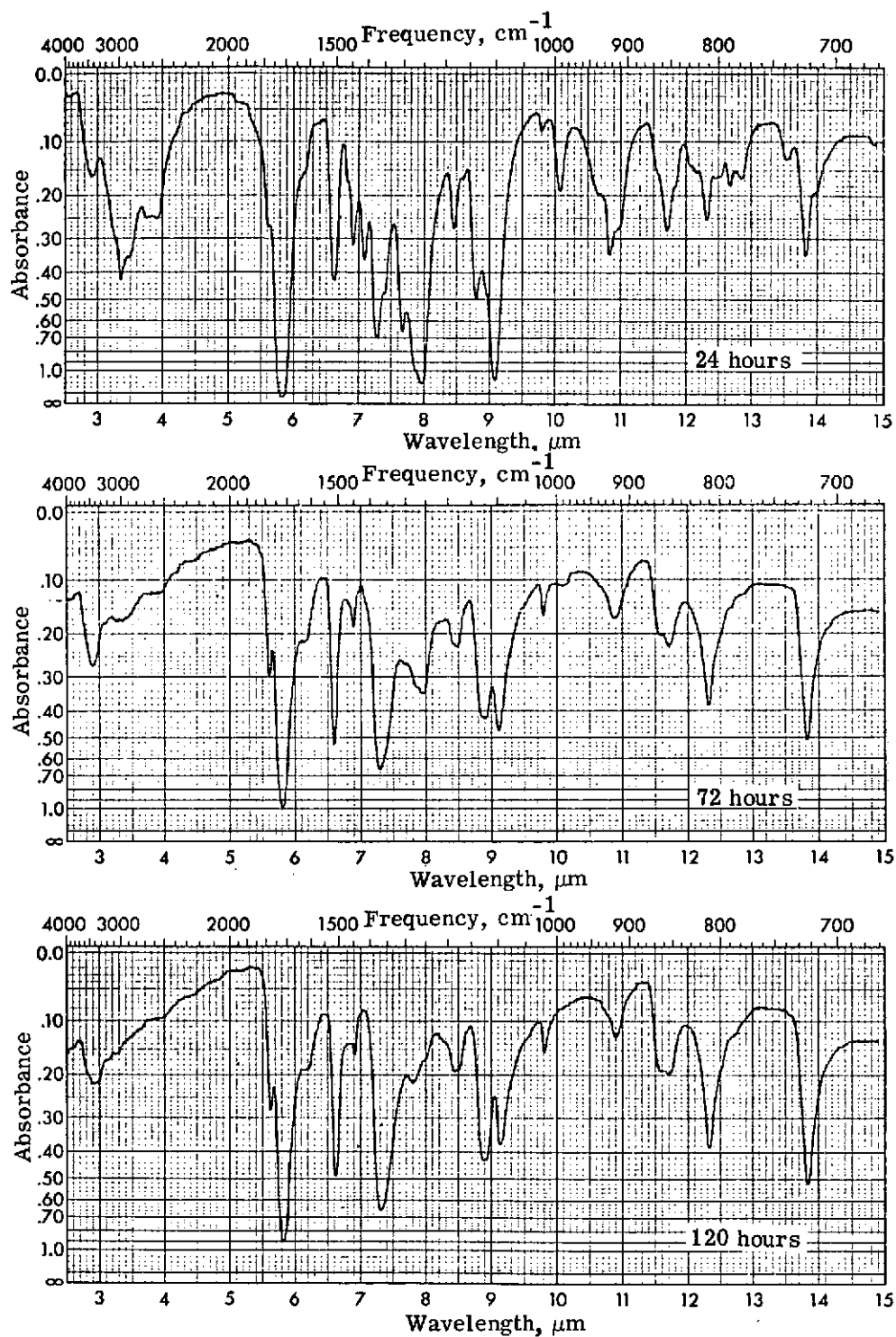


Figure 24.- Infrared spectra of meta open tube specimens annealed at  $170^{\circ}\text{C}$ .

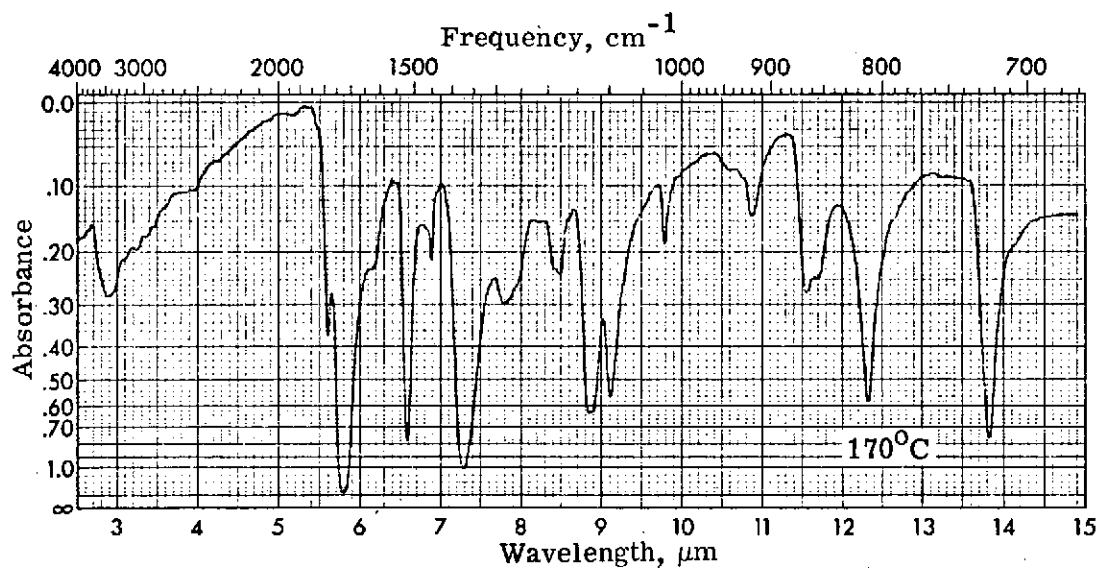
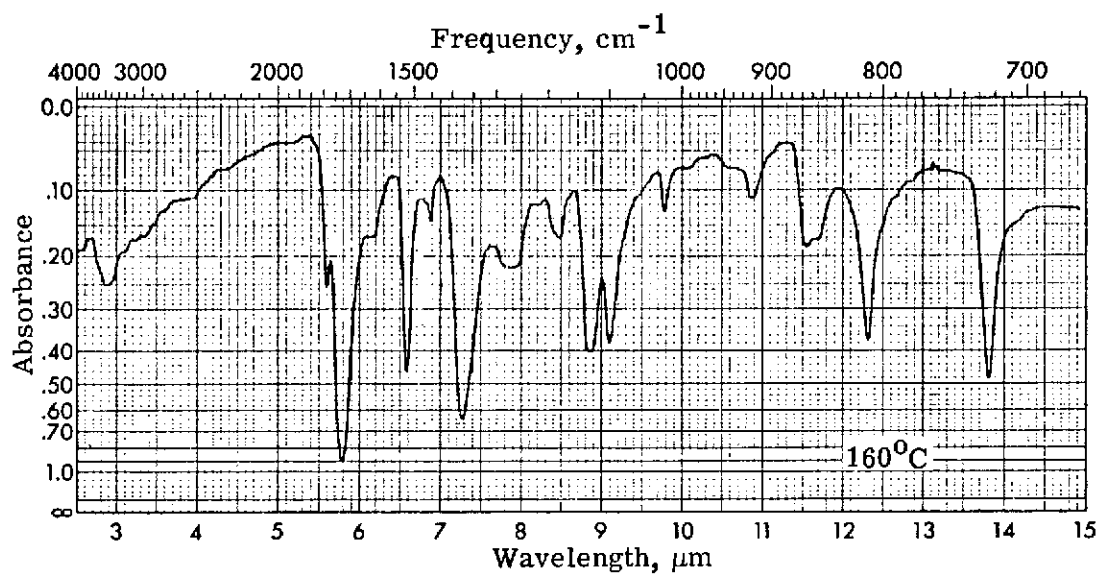


Figure 25.- Infrared spectra of meta sealed tube specimens annealed for 168 hours.

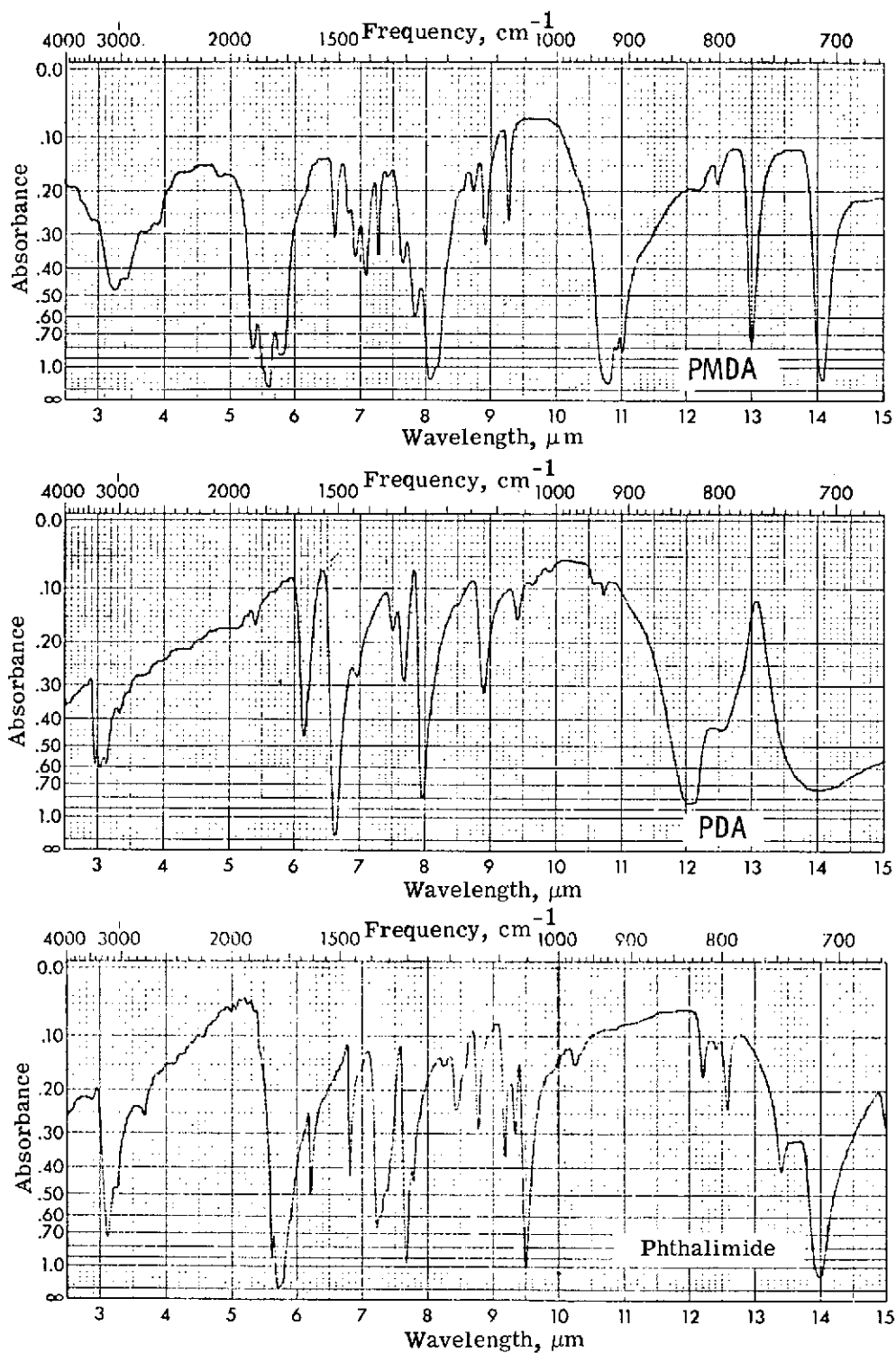


Figure 26.- Infrared spectra of selected compounds.

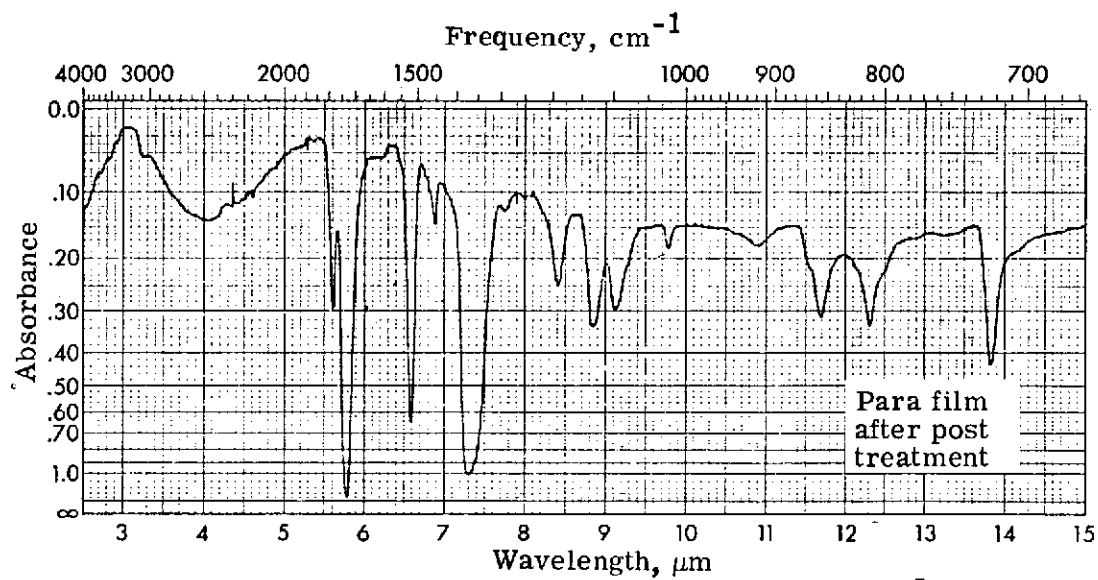
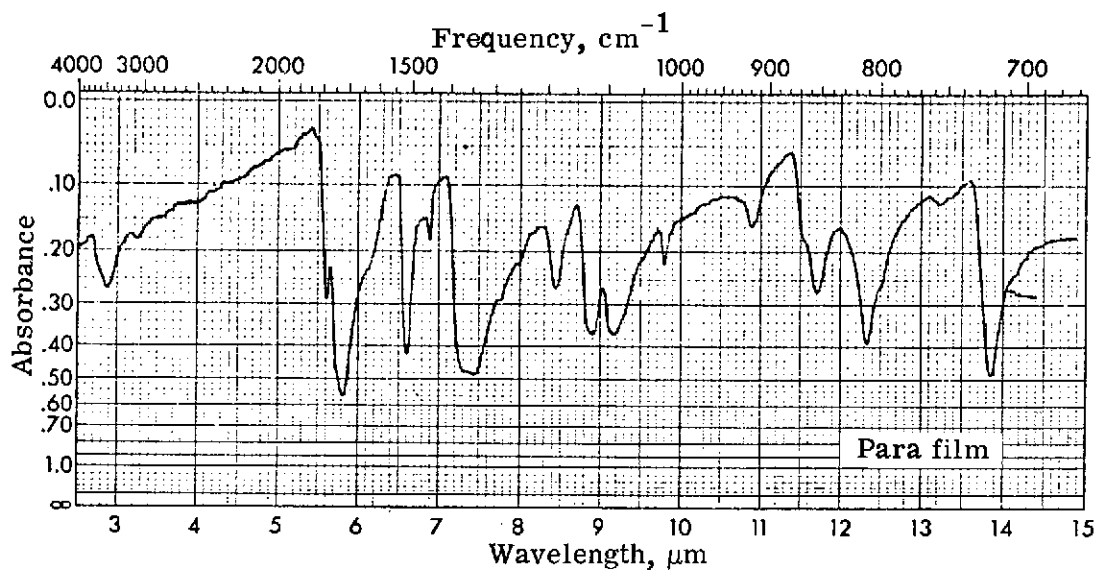


Figure 27.- Infrared spectra of solution made polymer.

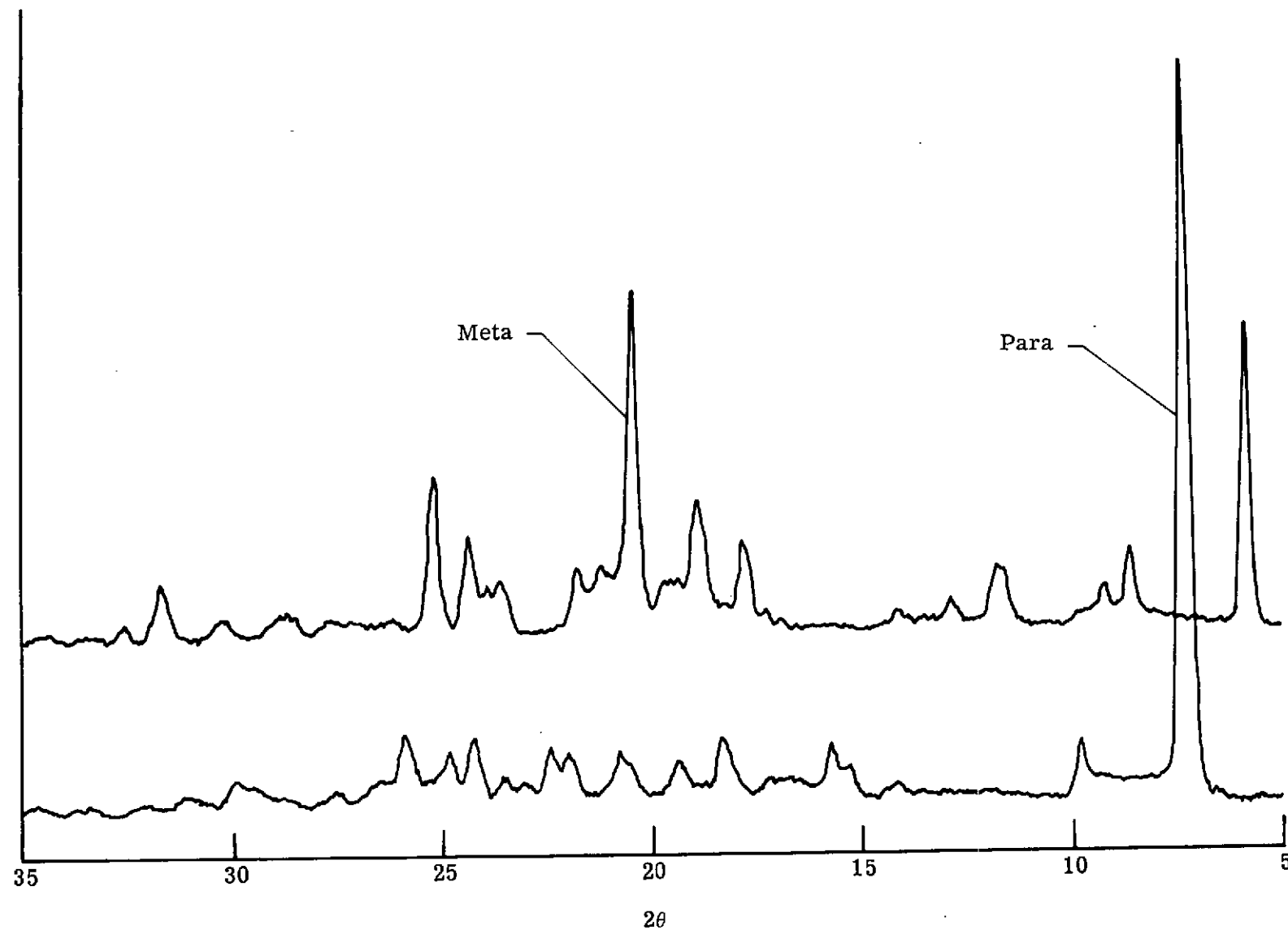


Figure 28.- X-ray powder diffractograms of specimens of para and meta isomers annealed at 170° C for 24 hours.



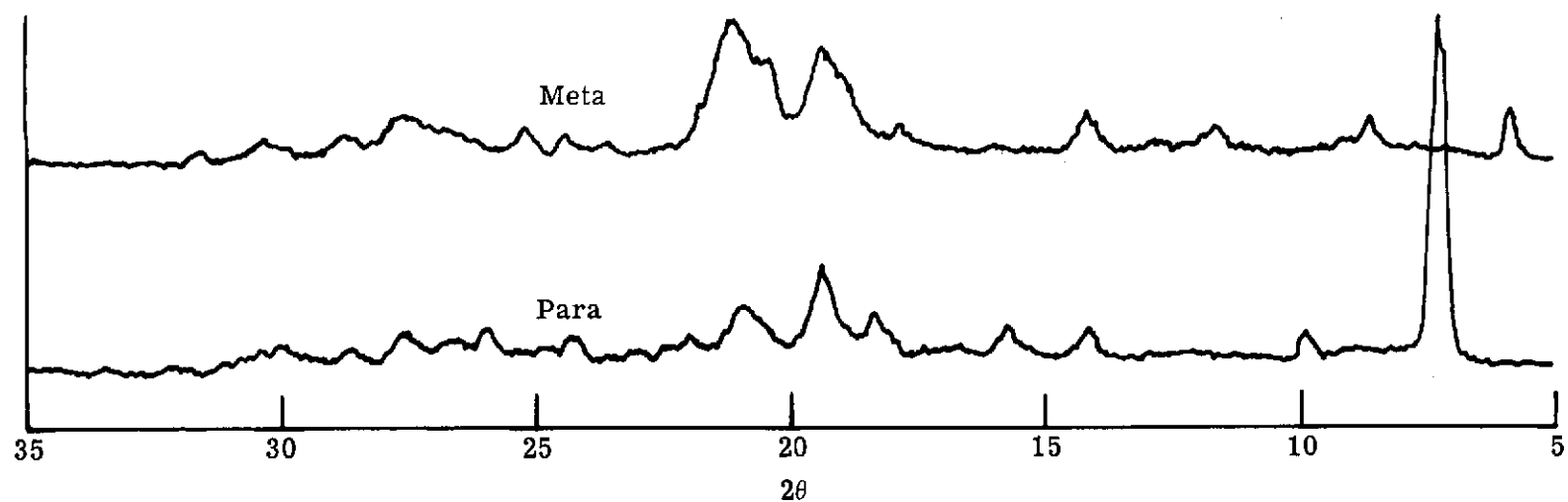
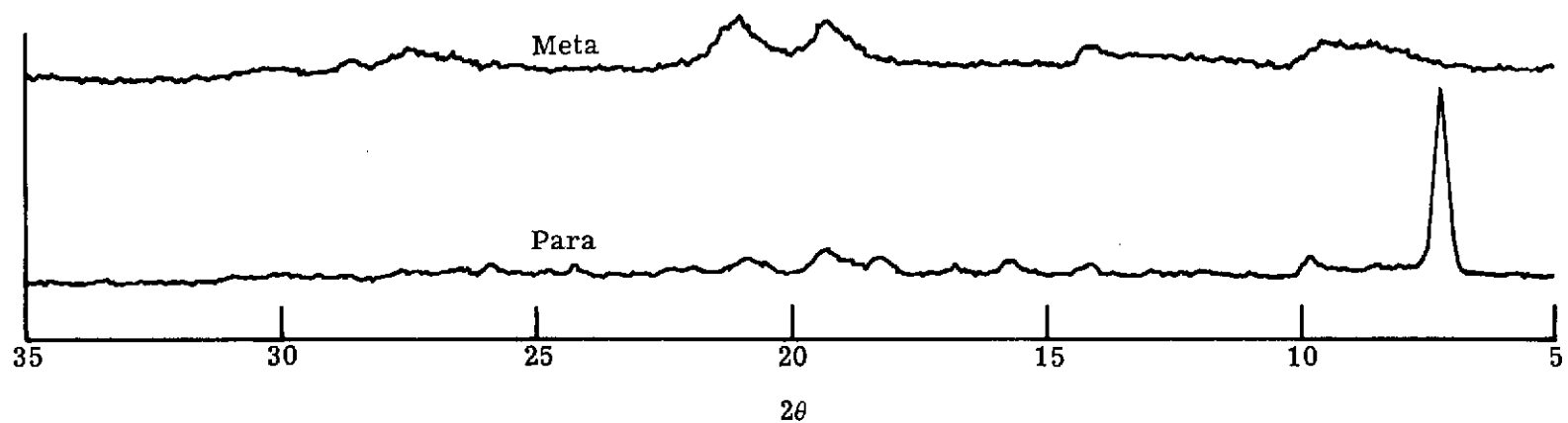


Figure 29.- X-ray powder diffractograms of specimens of para and meta isomers annealed at  $170^\circ\text{C}$  for 72 hours.



29 Figure 30.- X-ray powder diffractograms of specimens of para and meta isomers annealed at  $170^\circ\text{C}$  for 120 hours.

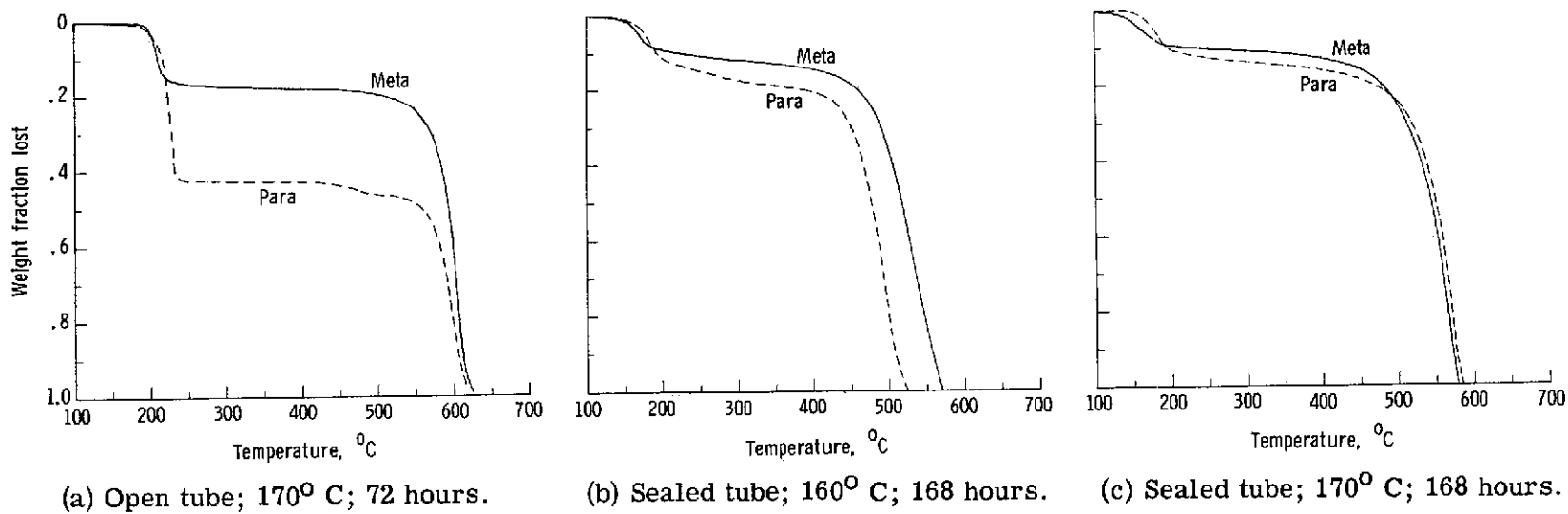


Figure 31.- Weight fraction lost as a function of temperature ( $^{\circ}\text{C}$ ) for meta and para specimens subjected to a static air TGA experiment with a heating rate of  $5\text{ }^{\circ}\text{C}/\text{min}$ .